A GEOMETRIC MORPHOMETRIC ANALYSIS OF THE PRIMATE PECTORAL GIRDLE

By

Kevin P. Klier

Committee:

Professor Noreen von Cramon-Taubadel, Chair

Assistant Professor Nicholas Holowka

Chapter One: Introduction

The clavicle, scapula, and humerus are the three bones that make up the tetrapod pectoral (shoulder) girdle and articulate together to perform important locomotor, feeding, grooming, and parenting functions. The pectoral girdle and the pelvic girdle are developmentally linked as analogous morphological structures (Agosto and Auerbach, 2022), although the pectoral girdle and associated fins evolved earlier in fish ancestors than the pelvic girdle (Sears et al., 2015). This is different from some other osteological structures such as forelimb and hindlimb bones, which are serially homologous. Examples of other serially homologous structures are vertebrae, ribs, and teeth and they can be described as special cases where developmental factors moderate covariation among structures (Young and Hallgrimsson, 2005). Past studies have suggested that the primate shoulder girdle is associated with differing functional demands that are imposed by variance in locomotion and posture (Larson, 2013). Therefore, clavicular, scapular, and humeral morphologies likely reflect taxonomic differences in locomotor repertoires (e.g., extent of brachiation capabilities) as well as differences in a species' social behaviors. These pectoral girdle functions are typically more variable than the functions that are associated with the pelvic girdle, as the forelimb is also involved in feeding, infant care, grooming, and carrying objects (Schmidt and Krause, 2010) all of which utilize the shoulder girdle in different ways. For example, different taxa display differing patterns of offspring care, which could potentially affect their shoulder girdle utilities during day-to-day life. Moreover, differences among the sexes in forelimb functions, especially related to feeding or infant care might also drive patterns of sexual dimorphism in the pectoral girdle. As such, a better understanding of the patterns of pectoral girdle morphology among taxa and among sexes would provide important insight into the evolutionary history of this skeletal region.

While a substantial amount of research has been conducted on the evolutionary morphology of the scapula (Bello-Hellegouarch et al., 2012; Green et al., 2016; Puschel and Sellers, 2016; Schmidt and Krause, 2010) and, to a lesser extent, the humerus (Arias-Martorell et al., 2015; Holliday and Friedl, 2013; Ki-Kydd and Piper, 2004; Yamanaka et al., 2005), there have been very few anthropological studies involving primate clavicles (although see Melillo et al. 2019; Squyres and DeLeon, 2015; Voisin, 2006). This is potentially due to the diminutive size of clavicles as well as their relative fragility, which likely prevents them from being studied as extensively as the other shoulder girdle bones. Clavicles are also relatively less morphologically complex, which may have resulted in less attention from osteological morphometricians. The primate clavicle functions as a strut that facilitates the structural connections between the sternum and scapulae (Squyres and Deleon, 2015) The clavicle essentially exists for the purpose of distancing the forelimbs from the thorax in a similar way that a mechanical crane requires a jib that distances the crane's mast from the moving trolly. In this example, the primate thorax is analogous to the crane's mast, the clavicle is the jib, and the humerus is the trolly (Bain et al., 2019). Primate clavicles are deeply involved in very different behaviors, which include infant handling and locomotion (Voisin, 2006). This raises the possibility of clavicular morphological differences, along with its relationship to the scapula and humerus, that are associated with taxonomic and/or functional differences amongst different primate species. Previous clavicular morphology research conducted by the author (Klier et al., 2021) produced results that suggested that, even though there was significant clavicular morphological overlap among certain catarrhine species, there was also a taxonomic signal associated with them.

Scapulae are substantial triangular blade-like bones that reside on the dorsal thorax, gliding over the dorsal ribs, and articulate with the proximal forelimbs at the glenohumeral joint (Aiello

and Dean 1990). Primate scapulae are much more morphologically complex than clavicles and are intricately involved in forelimb locomotor capabilities. Previous data have suggested that the functions of primate forelimbs have a significant effect on scapular morphology and that scapular morphology in quadrupedal primates seems to be more canalized than it is in other primate species that display suspensory behaviors (Young, 2006). Scapular research by Green and Alemseged (2012) investigated *Australopithecus afarensis* scapulae and concluded that they appear to share traits with climbing apes suggesting that they were potentially active climbers. Green et al. (2016) conducted a study concerning the scapular morphology of extant hominoids and the last common ancestor (LCA) of humans and African non-human apes and concluded that it would be reasonable to consider the human/African non-human ape LCA scapulae as being *gorilla*-like. While previous studies have focused on the relationship between scapular morphology and biomechanical function related to locomotion (e.g., Preuschoft et al., 2010; Taylor, 1997), recent studies (e.g., Young, 2008; Puschel and Sellers, 2016) have shown that scapular morphology also contains a substantial phylogenetic signal. Indeed, results from previous studies regarding primate scapulae have suggested that some aspects of the shoulder girdle potentially reflect phylogenetic relatedness that differs from functional patterns of variation. For example, research conducted by Taylor and Slice (2005) which involved the geometric morphometric analysis of chimpanzee and gorilla scapulae, concluded that there is no systematic pattern of differentiation that can predict different functions.

The humerus is the largest primate forelimb bone and has a humeral head at its proximal articulation with the glenoid fossa of the scapula, a diaphysis, and an irregular distal end that articulates with the ulna and radius (White and Folkens, 2005). Most primate shoulder girdle research that includes the humerus concentrates on the glenohumeral joint in order to better understand the relationship between the humerus and the scapula (Arias-Martorell, 2019). The

glenohumeral joint is the primary joint involved in forelimb locomotion and has increased mobility in the hominoids (Arias-Martorell, 2019). Hence, there is likely significant humeral morphological variance related to taxonomic signals in primates due to the significant diversity of primate locomotion patterns. For example, relative to other anthropoids, hominoid forelimbs are involved in quite disparate locomotion patterns (e.g., Young et al., 2010) including terrestrial knuckle-walking, ricochetal brachiation, and suspension, in contrast with human bipedalism that does not directly involve the pectoral girdle (Arias-Martorell, 2019). Therefore, while the link between overall humeral morphology (including cross-sectional geometry, e.g., Yamanaka et al., 2005) and modes of locomotion appears strong, it is less well understood to what extent the primate humerus also reflects the phylogenetic relationships among taxa.

Research investigating the morphological variance and integration of clavicles, scapulae, and humeri together has also been limited, but important complete primate shoulder girdle information can be derived from a small number of studies (Agosto and Auerbach, 2018; Agosto and Auerbach, 2022; Barros, 2014; Larson, 2013; Preuschoft et al., 2010). Similar to other primate osteological structures, many different avenues have been explored with different objectives in mind to research the shoulder girdle. This includes studies that concentrate on specific shoulder girdle structures such as the study by Sonnabend and Young (2009) that investigated the comparative anatomy of the rotator cuff's associated soft tissues, which are made up of four different muscles. The results suggested that the role of the rotator cuff's association with evolution parallels an anatomical adaptation to regular overhead locomotor movements and an increased requirement of forelimb utility from the sagittal plane (Sonnabend and Young 2009). Preushoft et al. (2010) conducted a functional analysis of the primate shoulder girdle from a biomechanical perspective. In both quadrupedal locomotion and suspension, the compression-resistant clavicles

facilitate distancing between the shoulder girdle and the thorax (Preushoft et al., 2010). Inuzuka (1992) also conducted research concerning shoulder girdle evolution with a concentration on the comparative functional morphology of the clavicle. The clavicular sternal epiphysis articulation is the last long bone to fuse and this delay in fusion may potentially allow for adjustment in growth of the clavicle to accommodate the morphology of the rest of the pectoral girdle (Inuzuka, 1992).

There have been other studies that focused on the complete shoulder girdle morphology of some new world monkeys such as the Cunningham (2005) study and another study conducted by Kagaya (2006). While Kagaya (2006) concentrated on the glenohumeral joint surface characteristics of three ateline new world monkeys *(Atele*, *Lagothrix*, and *Alouatta*), Cunningham (2005) concentrated on the foraging behaviors of *Cebus apella*, *Cebus albifrons*, *Saimiri sciureus*, *Pithecia pithecia*, and *Chiropotes Satanas*. *Cebus apella* was found to be morphologically similar to the other taxa, although differences in size was observable between (Cunningham, 2005). The other new world monkey study suggested that *Ateles* displays joint characteristics that are disparate from the other ateline species and are similar to *Hylobates* regarding its large breadth-length ratio of the glenoid surface and the humeral head, its comparatively orbicular humeral head morphology, and its dorsoventrally extensive humeral head relative to the glenoid surface (Kagaya, 2006).

Some primate shoulder girdle research, such as a study conducted by Chan (2008), has focused on different aspects of mobility such as passive arm circumduction, which is a combination of pectoral girdle and glenohumeral movements. Some of the findings include data revealing that Hylobatids appear to have the highest craniodorsal mobility amongst the species included in the study, but non-hylobatid hominoids have increased craniodorsal mobility relative to monkeys that are arboreal quadrupeds (Chan, 2008). Other anthropological shoulder girdle

research has investigated not only phylogenetic and functional morphology information but ontogenetic patterns as well. An ontogenetic study investigating the association between hominoid shoulder girdle morphology with functional factors and phylogeny, suggested the notion of an arboreal ancestor for the hominoid lineage and evidence of substantial parallel evolution of quadrupedalism in great apes (Barros, 2014). Other studies have focused on the comparison of shoulder girdle morphology between extant taxa and fossil hominins, with results suggesting that an *Australopithecus afarensis* (A.L. 288-1) displayed a mosaic of traits that appear to be similar to the *Homo* and *Pongo* genera and that *Australopithecus africanus* (Sts 7) shoulder morphology was more similar to arboreal apes that excluded *Homo sapiens* (Arias-Martorell et al., 2015).

An early study by Corrucini and Ciochon (1976) suggested that the morphological shoulder disparities between monkeys and apes and disparities between non-human apes and humans are associated with shoulder girdle muscular anatomy, which in all apes facilitates their feeding behavior and locomotor motions. Agosto and Auerbach (2018) conducted research involving constraints within the primate shoulder girdle as well as its overall patterns of integration and evolvability. They concluded that basicranial and shoulder girdle traits are not associated with evolutionary independence and that the basicranium and shoulder girdle are associated with evolutionary constraint. They have also suggested that the disparity in genetic covariance amongst different anatomical areas potentially contributed to the morphological variances amongst taxa that have been observed (Agosto and Auerbach, 2022). Therefore, taken together, previous research suggests that clavicular, scapular, and humeral morphologies may reflect gross taxonomic patterns as a function of shared phylogenetic history, irrespective of differences in the extent to which particular taxa travel arboreally or terrestrially, yet it is clear that functionally-mediated patterns of similarity and differences exist also. In order to address some of these gaps in

knowledge, this project set out to investigate several different hypotheses concerning clavicular, scapular, and humeral morphological similarities and differences within a sample of catarrhine parvorder taxa. Eight different catarrhine species were sampled that display a diversity of different behavioral and locomotor patterns. This included three old-world monkeys (*Cercopithecus ascanius*, *Macaca mulatta*, and *Trachypithecus cristatus*) and five ape (*Homo sapiens*, *Pan troglodytes*, *Gorilla gorilla*, *Pongo pygmaeus*, and *Hylobates lar*) taxa, that were specifically selected due to their varying modes of locomotion and diversity of social behaviors. *Cercopithecus ascanius* can be characterized as an arboreal quadruped (Gebo and Chapman, 1995), *Trachypithecus cristatus* is a mostly arboreal quadruped that is also considered a semi-brachiator (Harding, 2010), and *Macaca mulatta* is considered a semi-terrestrial quadruped (Vanhoof et al., 2020). One of the ape taxa, *Pongo pygmaeus*, use their arms and legs to elevate their bodies through the trees in a quadrumanous locomotion pattern (Strier, 2016). Two of the five ape taxa, *Gorilla gorilla* and *Pan troglodytes*, have a unique knuckle-walking mode of locomotion and have longer arms relative to their leg lengths, which facilitates an upright posture (Strier, 2016). *Hylobates lar* has a very unique form of locomotion and is considered an arboreal true-brachiator (Strier, 2016) which completely contrasts with the terrestrial bipedalism that is associated with *Homo sapiens*.

The aims of this research are to assess the extent to which pectoral girdle morphology (as seen in the shape of the clavicle, scapula, and humerus) reflects phylogenetic or functional differences among taxa due to shared patterns of ancestry and locomotory behavior. In addition, due to a lack of knowledge regarding patterns of sexual dimorphism in the catarrhine shoulder girdle (particularly for the clavicle), assessments of sexual dimorphism will be made among and within taxa. Previous research (Klier et al., 2021), it was found that *Trachypithecus cristatus* had substantial sexual shape dimorphism in the clavicle not found in other catarrhine taxa. Therefore,

it will be investigated whether this is also the case for the other pectoral girdle bones (Hypothesis 1_{A2}). Given the substantial difference in upper limb use in the true brachiating locomotion of gibbons relative to the generalized quadrupedal (or bipedal) locomotion of the other taxa, one alternate hypothesis will focus on testing whether morphological disparities (should they be found among taxa) lie only between *Hylobates lar* and other taxa or whether they are ubiquitous across all of the taxa sampled. Specifically, this thesis seeks to test the following null and alternative hypotheses:

$H1_0$: There is no intraspecific sexual shape dimorphism in the clavicle, scapula, or humerus

$H1_{A1}$: There is intraspecific sexual shape dimorphism in the clavicle, scapula, or humerus

$H1_{A2}$: There is sexual shape dimorphism in the clavicle, scapula, or humerus of *Trachypithecus cristatus* only.

$H2_0$: There is no interspecific shape disparity in the clavicle, scapula, or humerus

$H2_{A1}$: There is interspecific shape disparity in the clavicle, scapula, or humerus associated with phylogeny

$H2_{A2}$: There is interspecific shape disparity in the clavicle, scapula, or humerus associated with differences in locomotion

$H2_{A3}$: There is between species shape disparity in the clavicle, scapula, or humerus but only for *Hylobates lar*

Chapter Two: Materials and Methods

Materials

Sample

The dataset comprised clavicular, scapular, and humeral 3-dimensional (3D) surface scans for 233 individuals, totaling 699 bone specimens representing the shoulder girdle for a sample of catarhine primate taxa. Female and male individuals from eight different primate species were sampled, which included *Cercopithecus ascanius*, *Trachypithecus cristatus*, *Gorilla gorilla*, *Hylobates lar*, *Macaca mulatta*, *Pongo pygmaeus*, *Homo sapiens*, and *Pan troglodytes* (see Table 2.1). These eight catarhine parvorder species were selected for the purpose of observing potential osteological variation associated with multiple old-world monkeys and apes who have varying levels of sexual dimorphism and behavioral differences including differences in locomotor function. All of the specimens were collected from either the American Museum of Natural History in New York, the Neil C. Tappen Collection from the Department of Anthropology at the University of Minneapolis, the Cleveland Museum of Natural History Hamann-Todd Human and Non-Human Primate Osteological collections, the Harvard Museum of Comparative Zoology, the University at Buffalo Primate Skeletal collection, or the Field Museum of Chicago, Illinois (Table 2.1). The sex of each individual was verified by collection tag examinations as well as a visual inspection of the individual's canine morphology. The 3D scans used during this research project were collected by multiple different researchers (Table 2.1) who support an ongoing skeletal analysis project for the Buffalo Human Evolutionary Morphology Laboratory (BHEML). However, all post-collection landmarking and processing was conducted by the author.

In order to correlate the clavicular, scapular, and humeral variance data with known genetic data, a genetic distance matrix was created and processed in PAST 4.09 (Hammer, O., Harper, D.A.T., P.D. 2001) and PASSaGE 2 (Rosenberg, M.S., and C.D. Anderson, 2011). The genetic distance matrix was derived from a molecular phylogenetic tree and a table displaying taxonomic branch length calculations that were developed by Perelman et al. (2011) and was used to calculate the specific genetic relatedness among the eight different catarrhine species included in this project. A description of the data sourcing and development is explained in the materials section below.

Methods

Data Collection

Scanning/Aligning procedures

All of the 3D scans used were captured using an HDI Advance high-definition 3D scanner (LMI Technologies Inc., Vancouver, Canada) that was consistently calibrated each time a new specimen was scanned. First, all appropriate connections for the computer, tray, and scanner were performed prior to 3D image capture procedures. Each individual bone was held in place by an appropriate amount of putty and firmly placed on a rotating steel plate (tray) that resided on a sturdy, level laboratory bench to ensure that stability was sufficient for 3D image capture. Different amounts of putty were tailored respective to the size, weight, and shape of the different bones that were being scanned. For example, different amounts of putty were required to stabilize the clavicles of *Macaca mulatta* compared to the amounts of putty that were needed to hold *Gorilla gorilla* humeri. Post initial image capture, each specimen was placed exactly 180 degrees in the opposite direction so that the alternative side could be captured as well. After all images were satisfactorily captured, they were recombined in an alignment procedure utilizing FlexScan 3D software (Polyga, 2021). The alignment procedure is necessary in order to obtain a complete digitized 3D image that would subsequently be stored as a Polygon File Format (PLY) file on a laboratory computer for additional processing.

Table 2.1. Study sample, indicating the sex distribution of each taxon plus the repositories where the samples are housed.

Species	***Male***	***Female***	***Museums***[1]	***Researchers (scan collection)***
Cercopithecus ascanius	11	13	AMNH/NCT	Brittany Kenyon-Flatt
Trachypithecus cristatus	16	16	FMNH/MCZ	Brittany Kenyon-Flatt/Evan Simons
Gorilla gorilla	16	12	CMNH/MCZ	Marianne Cooper/Evan Simons
Hylobates lar	19	26	MCZ	Marianne Cooper/Evan Simons
Macaca mulatta	14	12	UBPSC	Kevin Klier/Evan Simons
Pongo pygmaeus	3	4	CMNH/MCZ	Marianne Cooper/Evan Simons
Homo sapiens	29	19	CMNH	Amandine Eriksen./Marianne Cooper/Evan Simons
Pan troglodytes	12	11	AMNH/CMNH/MCZ	Marianne Cooper/Evan Simons
Total	120	113		

[1]American Museum of Natural History (AMNH), Neil C. Tappen Collection, Department of Anthropology, University of Minneapolis (NCT), Field Museum of Natural History (FMNH), Harvard Museum of Comparative Zoology (MCZ), University at Buffalo Primate Skeletal Collection (UBPSC), Cleveland Museum of Natural History (CMNH).

Landmarking Procedure

Once all scans were aligned and saved as PLY files, a single observer (Kevin P. Klier) superimposed digital landmarks on all images utilizing previously established landmarking methods developed by Melillo et al. (2019) for the clavicles, Green et al. (2016) and Young (2008) for the scapulae with modifications by Conaway (2020), and Holliday & Friedl (2013) for the humeri with modification by Conaway (2020). IDAV Visualization and Graphics Research Group's Landmark 3.6 software (Wiley, 2006) was utilized to place and record all 3D landmark coordinates for each specimen. A project was created in Landmark 3.6 (Wiley, 2006) for each species' shoulder bones (clavicles, scapulae, and humeri) which amounted to 24 individual projects containing an accumulation of 699 3D images. Each specimen was subsequently loaded from each project into the program's windowpane for individual landmark superimpositions which would later be exported as a (.dta) file to the laboratory computer for further analyses. Examples of post landmarked 3D clavicular scans from the sternal and acromial articulations are illustrated in Figure 2.1. Examples of post landmarked 3D scapular scans from the posterior, anterior and lateral sides are portrayed in Figure 2.2, while examples of post landmarked 3D humeral scans from the posterior, anterior, medial, and lateral sides are shown in Figure 2.3.

Table 2.2. Clavicle anatomical landmarking protocol (Melillo et al., 2019) that was applied to the study sample (see Table 2.1).

Landmark No.	Name	Description
CL1	Anterior sternal end	Anterior extent of the sternal articulation.
CL2	Posterior sternal end	Posterior extent of the sternal articulation.
CL3	Conoid tubercle	Inferior-most projection of the conoid tubercle.
CL4	Anterior acromial end	Anterior extent of the acromial articulation.
CL5	Posterior acromial end	Posterior extent of the acromial articulation.
CL6	Midline sternal end	The intersection of the midline curve and the external surface of the sternal end.
CL7	Midline acromial end	The intersection of the midline curve and the external surface of the acromial end.

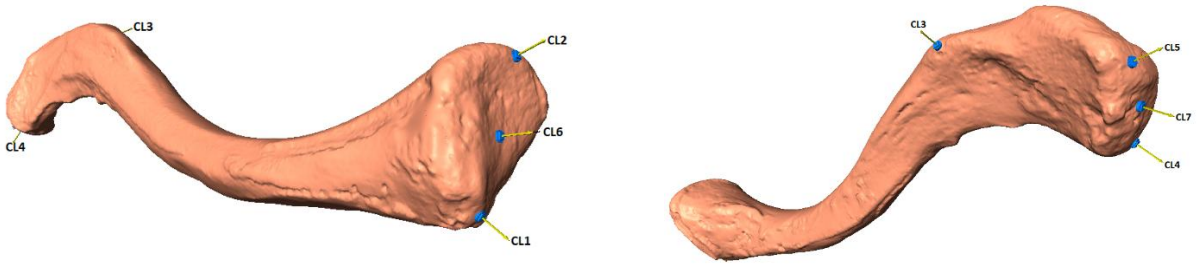

A **B.**

Figure 2.1. Clavicle landmarks viewed from the sternal end (A) and acromial end (B).

Table 2.3. Scapula anatomical landmarking protocol. Adapted from Green et al. (2016), Young (2008), and Conaway (2020). An asterisk (*) indicates a landmark that was removed for this project.

Landmark No.	Name	Description
1	Suprascapular notch	Most inferior point of the suprascapular notch.
2	Superior angle	Most extreme point of the superior angle.
3	Spine-medial border intersection	Most medial extent of a line drawn from the point where the scapular spine intersects with the scapular blade.
4	Inferior angle	Most extreme point of the inferior angle.
5	Infraglenoid tubercle	Infraglenoid tubercle.
6	Spinoglenoid notch	Spinoglenoid notch.
7	Glenoid fossa inferior	Most inferior point of the glenoid fossa.
8	Glenoid fossa anterior	Most anterior point of the glenoid fossa.
9	Glenoid fossa posterior	Most posterior point of the glenoid fossa.
10	Glenoid fossa superior	Most superior point of the glenoid fossa.
11	Coracoid process superior	Most superior point of the coracoid process.
12	Coracoid process inferior	Most inferior point of the coracoid process.
13	Acromion process	Most distal (lateral) point of the acromion.
*14	Teres major fossa	Lateral projection of the Teres major fossa.

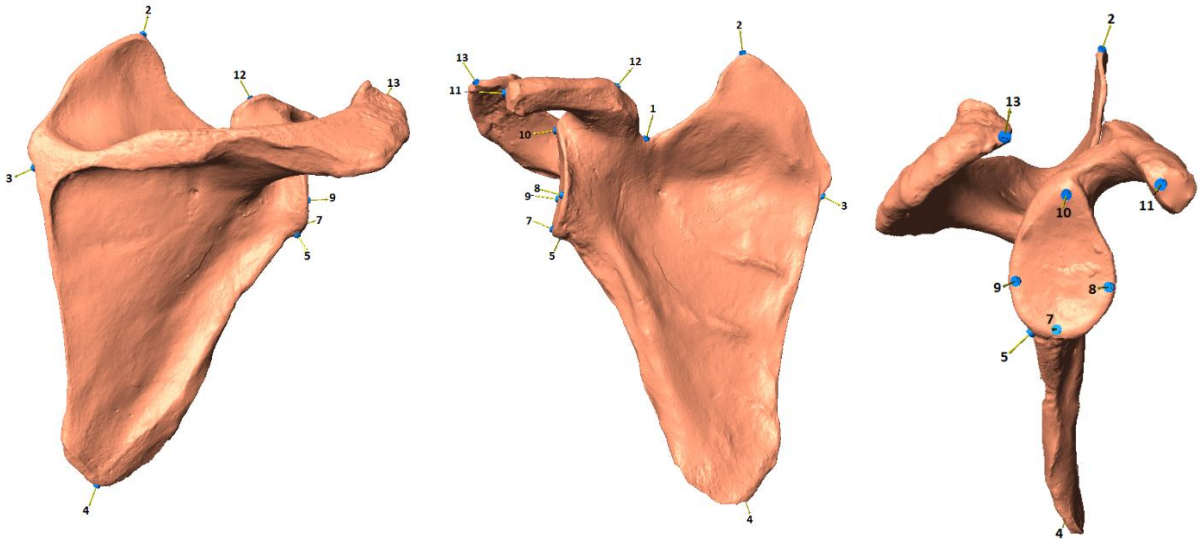

A **B** **C**

Figure 2.2. Scapula landmarks viewed from the posterior side (A), the anterior side (B), and the lateral side (C).

Table 2.4. Humerus anatomical landmarking protocol. Adapted from Holliday & Friedl (2013) and Conaway (2020). An asterisk (*) indicates a landmark that was removed for this project.

Landmark No.	Name	Description
1	Humeral head	Center of humeral head.
2	Inferior insertion	Most inferior point of the head-neck intersection.
3	Lateral insertion	Most lateral point of the head-neck intersection.
4	Medial insertion	Most medial point of the head-neck intersection.
5	Superior greater tubercle	Most superior point of the greater tubercle.
6	Lateral greater tubercle	Most lateral point of the greater tubercle.
7	Superior lesser tubercle	Most superior point of the lesser tubercle.
8	Medial lesser tubercle	Most medial point of the lesser tubercle.
9	Medial epicondyle	Most medial point of the medial epicondyle.
10	Lateral epicondyle	Most lateral point of the lateral epicondyle.
11	Distal Capitulum	Most distal point of the capitulum-epicondyle juncture.
12	Anterior Capitulum	Most anterior point of the capitulum-epicondyle juncture.
13	Posterior Capitulum	Most posterior point of the capitulum-epicondyle juncture.
14	Distal trochlea	Most distal point of the trochlea-epicondyle juncture.
15	Anterior trochlea	Most anterior point of the trochlea-epicondyle juncture.
16	Posterior Trochlea	Most posterior point of the trochlea-epicondyle juncture.
*17	Deltoid tuberosity	Most lateral point of the deltoid tuberosity.
*18	Intertubercular groove	Most anterolateral point of the intertubercular groove.

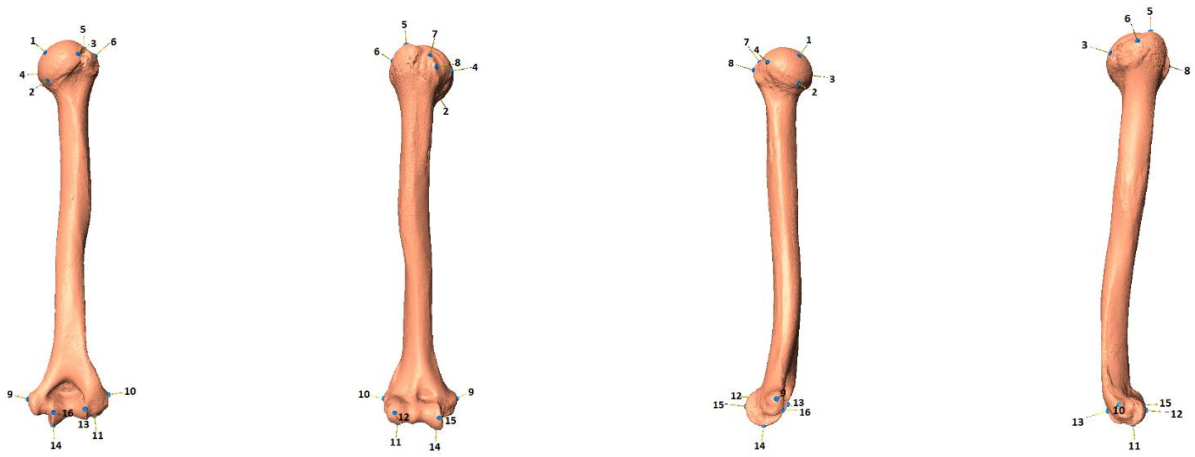

A **B** **C** **D**

Figure 2.3. Humerus landmarks viewed from the posterior side (A), the anterior side (B), the medial side (C), and the lateral side (D)

A total of seven landmarks were superimposed on each 3D clavicle image and were labeled CL1 through CL7 corresponding to their associated osteological structures (see Table 2.2; Melillo et al., 2019). A total of 13 landmarks were superimposed on each 3D scapula image as established by Green et al. (2016) and Young (2008). The 14th landmark from the original protocol, representing the Teres major fossa, was omitted due to location identification complications as established by a modification developed by Conaway (2020). Additionally, the order of landmarks seven through ten were reordered from the original protocol to facilitate processual efficiency (see Table 2.3). A total of 16 landmarks were superimposed on each 3D humerus image as established by Holliday & Friedl (2013) and modified by Conaway (2020) (see Table 2.4).

Post osteological specimen 3D image landmarking completion, each specimen was re-examined to ensure that all landmarks were accurately and appropriately recorded corresponding to their correct locations. Occasionally, anomalies were detected and identified during the post processing quality control procedure. In each of these incidences, there were either problems with missing landmarks or the landmarks were placed in inaccurate locations on the 3D images themselves during the landmarking process in Landmark 3.6 (Wiley, 2006). Any and all discrepancies were subsequently investigated and corrected to ensure the minimization of any data inaccuracies that could potentially compromise the integrity of the analytical results. Post quality control procedure, all seven clavicular, all 13 scapular, and all 16 humeral landmarks were collected and recorded for all specimens used during this research.

Analytical Methods

Generalized Procrustes Analysis/Procrustes Distances

All of the individual specimen names along with their associated landmark coordinates were used as input to create a Morphologika style file for each bone category. The three Morphologika style files were each individually uploaded into MorphoJ (Klingenberg, 2011), which was used to perform all of the geometric morphometric analyses. In order to register the landmark data for each shoulder girdle bone, a generalized Procrustes analysis (GPA) was performed in MorphoJ (Klingenberg, 2011) separately for each bone. GPA superimposes separate similar objects (landmark configurations) based on their geometric centers which are called centroids. After the structures are superimposed on one another, they are all scaled to the same centroid sizes in order to exclude the effect of size as a variable in the analysis. After this, the GPA rotates all of the different configurations in order to get all of their equivalent associated landmarks in as close proximity to each other as possible (Baab et al., 2012). Post GPA function, it is now possible for the superimposed structures to be understood as a single point in a high-dimensional shape space. This is necessary because morphologies can only be compared once scale, orientation, and location are removed as potential confounding variables. Then Procrustes distances are quantified in order to measure the differences in morphological variation among specimens. A Procrustes distance is established by taking the square root of the sum of all squared distances associated with corresponding landmarks, and is the standard measurement of morphological variation among specimens in Procrustes-based geometric morphometrics (Baab et al., 2012). In the case of the current project, average Procrustes distances among taxa were extracted as a pairwise taxon matrix for further comparison of morphological disparity.

Data Visualization

In order to produce a general visualization of the clavicular, scapular, and humeral morphological variability associated with the eight different species included in this study, a Principal Components Analysis (PCA) was performed in MorphoJ (Klingenberg, 2011) based on the total covariance matrix of the GPA-aligned coordinates. A separate PCA was performed for each shoulder girdle bone to visualize osteological morphological disparities amongst the different taxa. A PCA displays a 2D (2-dimensional) visualization of data spaces that have higher dimensionalities. The PCA does this by rotating a data space into a group of orthogonal axes that are associated with ever decreasing amounts of overall variation. Therefore, the first PC axis (PC1) explains the most variances, PC2 the second most, and so on. Generally speaking, any major shape differences among taxa will be revealed by plotting the positions of specimens on the first few PC axes. PCAs do not produce statistical results *per se* but do serve as a useful visualization technique for evaluating morphological differences within- and between samples.

Sexual Dimorphism

In order to test for the presence of sexual dimorphism within and among species (Hypothesis one), a series of Procrustes ANOVAs were conducted in, MorphoJ (Klingenberg, 2011). First a Procrustes ANOVA was run on all taxa simultaneously to assess if there were any significant shape differences between males and females. As this result was significant, a series of Procrustes ANOVAs were conducted separately for each bone for each species to assess which taxa were sexually dimorphic and which were not. Once each bone for each species was analyzed for sexual dimorphism, they could all be compared with each other in order to understand which, if any, species were sexually dimorphic in shoulder girdle shape.

Shape Differences Amongst Taxa

To quantify the level of clavicular, scapular, and humeral morphological variation amongst species, a Canonical Variate Analysis (CVA) was performed using MorphoJ (Klingenberg, 2011) to test for significant differences among taxa based on Procrustes distance, using a permutation test with 10,000 iterations. The permutation procedure takes all of the different individual specimens and shuffles them so that they are no longer associated within their discrete categories (species in this case). After the specimens have been shuffled, the permutation procedure performs another calculation of the difference in means of the Procrustes distances. The permutation procedure allows researchers to understand if the morphological differences among species are simply due to chance or if they are truly statistically significant. This statistical procedure was used to test the predictions of Hypothesis 2 regarding morphological disparity among taxa. The clavicular, scapular, and humeral Procrustes distance matrices were subsequently uploaded into PAST 4.09 (Hammer, O., Harper, D.A.T., P.D. 2001) to perform a Non-metric Multidimensional Scaling (MDS) procedure to produce a 2-dimensional (2D) plot of the average differences between taxa.

Locomotion

The species included in this research project vary substantially in their positional and locomotor behaviors. For example, *Pan troglodytes* and *Gorilla gorilla* tend to engage in knuckle-walking, *Hylobates lar* is associated with true brachiation, and some of the other species are arboreal or terrestrial quadrupeds. In order take these different species' locomotion into consideration a locomotor similarity scoring system was developed (see Table 2.5). Each species was given two types of scores – a "loading" score to reflect which limbs are most used when moving, and a "gravity" score to reflect the degree of arboreality. Loading scores were numbered

one through five and represent whether or not a particular species primarily uses their forelimbs, hindlimbs, or all four limbs during locomotion. The gravity scores are numbered one through five as well and are representative of varying degrees between terrestrial and arboreal locomotion. Table 2.5. illustrates the scoring system and relative positions of all the species considered here. Post loading and gravity score attribution, a matrix was produced that displays differences in the distances between the different species based on their scores. The produced matrix was subsequently uploaded into Past 4.09 (Hammer, O., Harper, D.A.T., P.D., 2001) for a Non-metric Multidimensional Scaling (MDS) procedure which provided a two-axis scatter plot.

Cercopithecus ascanius was assigned a loading score of three due to its quadrupedal mode of locomotion and was assigned a gravity score of four due to its propensity to travel arboreally. *Trachypithecus cristatus* was assigned a loading score of three due to its quadrupedal mode of locomotion and was assigned a gravity score of five due to its near exclusive arboreal mode of locomotion. *Gorilla gorilla* was assigned a loading score of 2.5 due to its knuckle walking mode of locomotion and was assigned a gravity score of one due to its nearly exclusive terrestrial mode of locomotion. *Hylobates lar* was assigned a loading score of one due to its unique true brachiation mode of locomotion and was assigned a gravity score of five due to its nearly exclusive arboreal mode of locomotion. *Macaca mulatta* was assigned a loading score of three due to its quadrupedal mode of locomotion and was assigned a gravity score of three due to its intermediated arboreal and terrestrial mode of locomotion. *Pongo pygmaeus* was assigned a loading score of two due to its intermediate association with both two limb and four limb modes of locomotion and was assigned a gravity score of four due to its propensity to locomote arboreally, but can also locomote terrestrial some of the time. *Homo sapiens* were assigned a loading score of five due to its unique bipedal mode of locomotion and was assigned a gravity

score of one due to its exclusive association with terrestrial locomotion. Finally, *Pan troglodytes* was assigned a loading score of 2.5 due to its knuckle walking mode of locomotion and was assigned a gravity score of two due to its association with terrestrial locomotion as well as being able to travel arboreally some of the time. These two values were used to generate an among-taxon locomotion distance matrix based on the Euclidean distances among all pairs of taxa.

Table 2.5. Locomotion scores.

							Gravity score
	Hylobates lar		*Trachypithecus cristatus*			Arboreal	5
		Pongo pygmaeus	*Cercopithecus ascanius*				4
			Macaca mulatta				3
			Pan troglodytes				2
			Gorilla gorilla		*Homo sapiens*	Terrestrial	1
Loading score	Two Forelimbs		Four Limbs		Two Hindlimbs		
	1	2	3	4	5		

Genetic Distance

Phylogenetic distances were calculated among each of the species on a pairwise basis by adding each of the individual branch lengths back to the node of common ancestry between two taxa, based on the maximum likelihood branch lengths published by Perelman et al. (2011). The research data was established from molecular phylogeny derived from 34,927 base pair (bp) of sequence and was amplified from 54 nuclear genes from 191 different species (Perelman et al.,

2011). Once all of the different genetic distances were calculated for each of the pairs of primate species based on the molecular phylogeny data, a matrix was created that represented the genetic distances among all taxa. The produced matrix was then subsequently uploaded into Past 4.09 (Hammer, O., Harper, D.A.T., P.D., 2001) for a Non-metric Multidimensional Scaling (MDS) procedure which provided a two-axis scatter plot. A neighbor-joining tree was also created in PAST 4.09 (Hammer, O., Harper, D.A.T., P.D., 2001) from the genetic distance matrix to allow for a visual representation of the genetic relatedness of all species and to verify that the genetic distance matrix returned the correct phylogenetic tree topography.

Correlation Procedures

The pairwise taxon distances matrices representing genetics, locomotion, and morphological disparity for the three shoulder girdle bones were uploaded into PASSaGE 2 (Rosenberg, M.S., and C.D. Anderson, 2011) and were subjected to a series of Mantel and partial Mantel tests (Mantel, 1967) to assess the strength of correlation among these different measures of taxon disparity. Mantel tests were first used to reveal the overall correlations between the genetic distance matrix and the clavicular, scapular, and humeral variation matrices individually to test the predictions of Hypothesis 2A. Then, Mantel tests were used to reveal the overall correlations between the locomotion distance matrix and the clavicular, scapular, and humeral variation matrices individually to test the predictions of Hypothesis 2B. Finally, partial Mantel tests were performed by analyzing correlations between the locomotion distance matrix and all three-shoulder girdle bone variation distances while holding the genetic distance matrix as a constant. This was designed to test whether any significant associations between morphology and locomotion remained once genetic relatedness (phylogeny) was accounted for. These Mantel tests were all performed with a 999 replicate permutation test that produced two-tailed test results.

Chapter Three: Results

Data Visualization

The results from the principal components analyses for the clavicles, scapulae, and humeri can be seen below in Figures 3.1, 3.2, and 3.3. The first principal component is on the x-axis and the second principal component is on the y-axis for each of the three PCA plots and were specifically chosen because they represent most of the variation that exists for each of the three shoulder girdle bones. There appears to be some degree of taxonomic separation for all three shoulder girdle bones, but much less for the clavicles compared to the scapulae and humeri.

For the clavicles, the first principal component accounts for 43.45% of total variance and the second principal component accounts for 20.89% of total variance. The wireframe diagrams representing the shape transformations along PC1 and PC2 suggest that the majority of the clavicular shape variation is associated with the distance between the conoid tubercle and the acromial articulation (Fig. 3.1). In the case of the clavicle, PC1 separates the gibbons from humans, with *Pongo* falling closer to the gibbons and the other African apes intermediate. There is also some separation between the cercopithecines and the colobines on PC1. On PC2, there is some separation between gorillas and other taxa, although differences among taxa based on their taxonomic affiliation are not obvious (Fig. 3.1).

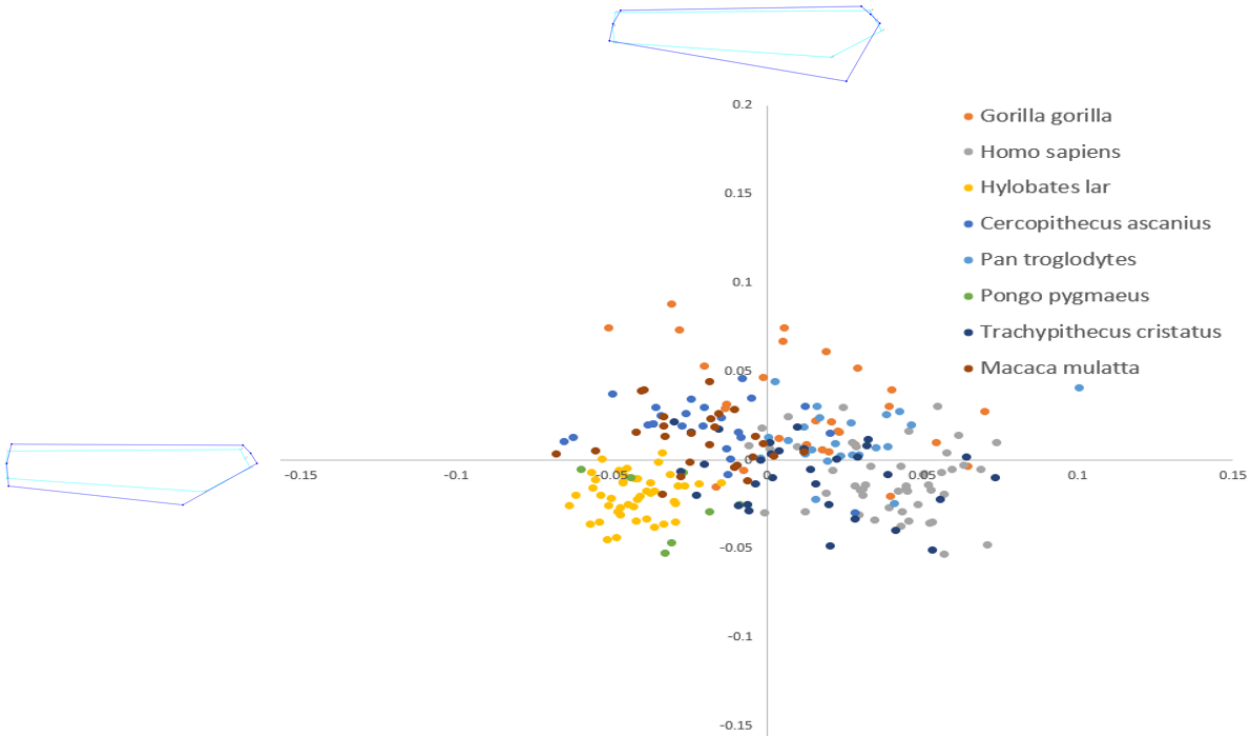

Figure 3.1. Interspecific clavicular morphological variation PCA plot with wireframes, illustrating the major shape changes along each of the PCs. PC1 (x-axis) explains 43.45% of the variance, while PC2 (y-axis) explains 20.89% of the variance. The light blue wireframe illustrates the average shape transformation towards the negative end, while the dark blue wireframe illustrates the average shape towards the positive end.

For the scapulae, the first principal component accounts for 45% of total variance and the second principal component accounts for 26.66% of total variance. The scapular variance represented by PC1 appears to be associated with the position of the inferior angle, while PC2 appears to be associated with the position of the superior angle and the spine-medial border intersection (Fig. 3.2), PC1 clearly separates the gibbons from the large-bodied apes, with humans being the most different from the gibbons. All other apes are somewhat intermediate, although PC2 distinguishes between *Pongo pygmaeus* and the chimpanzees and gorillas. However, it should be recognized that *Pongo pygmaeus* has a much smaller sample size than the rest of the species

do. PC2 also clearly distinguishes the cercopithecoid taxa from the ape taxa, while macaques are separated from *Cercopithecus* and *Trachypithecus* on PC1.

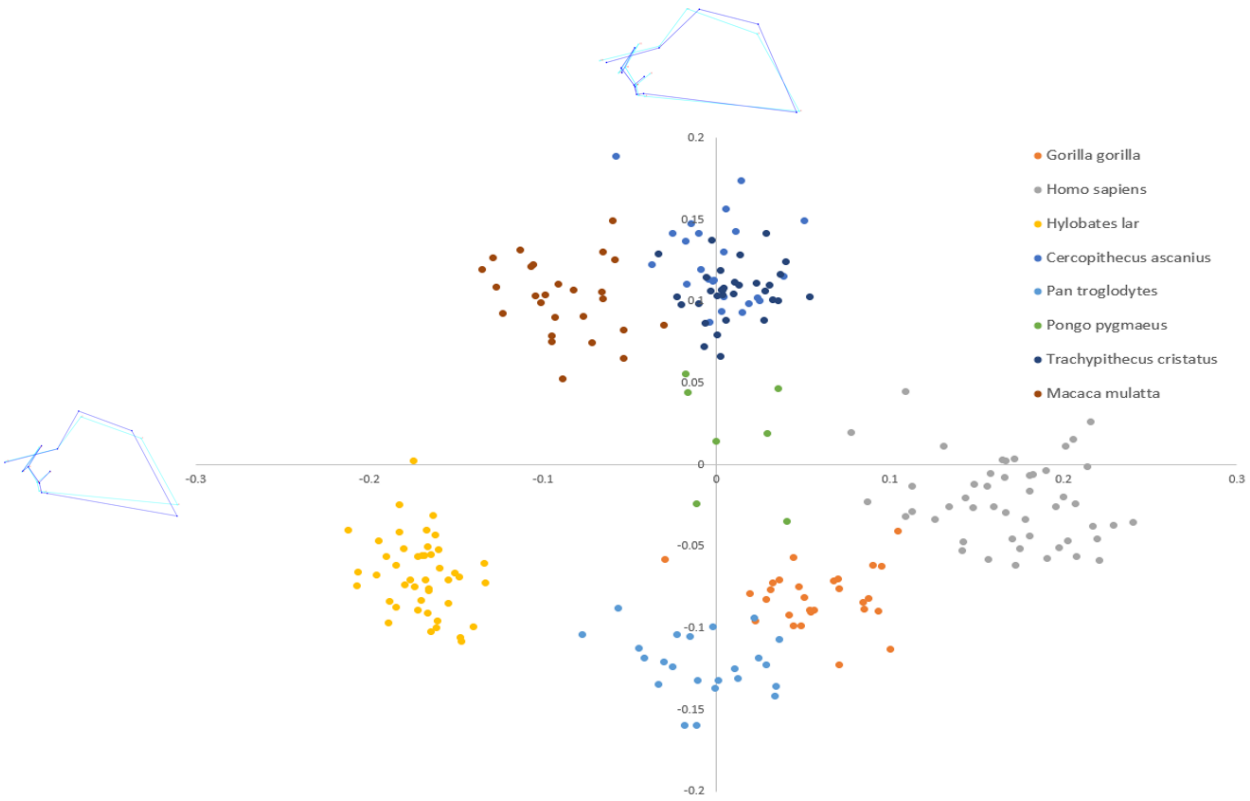

Figure 3.2. Interspecific scapular morphological variation PCA plot with wireframes, illustrating the major shape changes along each of the PCs. PC1 (x-axis) explains 45% of the variance, while PC2 (y-axis) explains 26.66% of the variance. The light blue wireframe illustrates the average shape transformation towards the negative end, while the dark blue wireframe illustrates the average shape towards the positive end.

Finally, for the humeri, the first principal component accounts for 55.18% of total variance and the second principal component accounts for 22.91% of total variance. The humeral variance represented by PC1 appears to be associated with the narrowness of the shaft as it approaches the distal end, while PC2 appears to be associated with the humeral shaft curvature (Fig. 3.3.) PC1 distinguishes between three groups of taxa, one containing all apes except for gibbons, one containing the monkey taxa, while *Hylobates lar* is completely separated from all the other species.

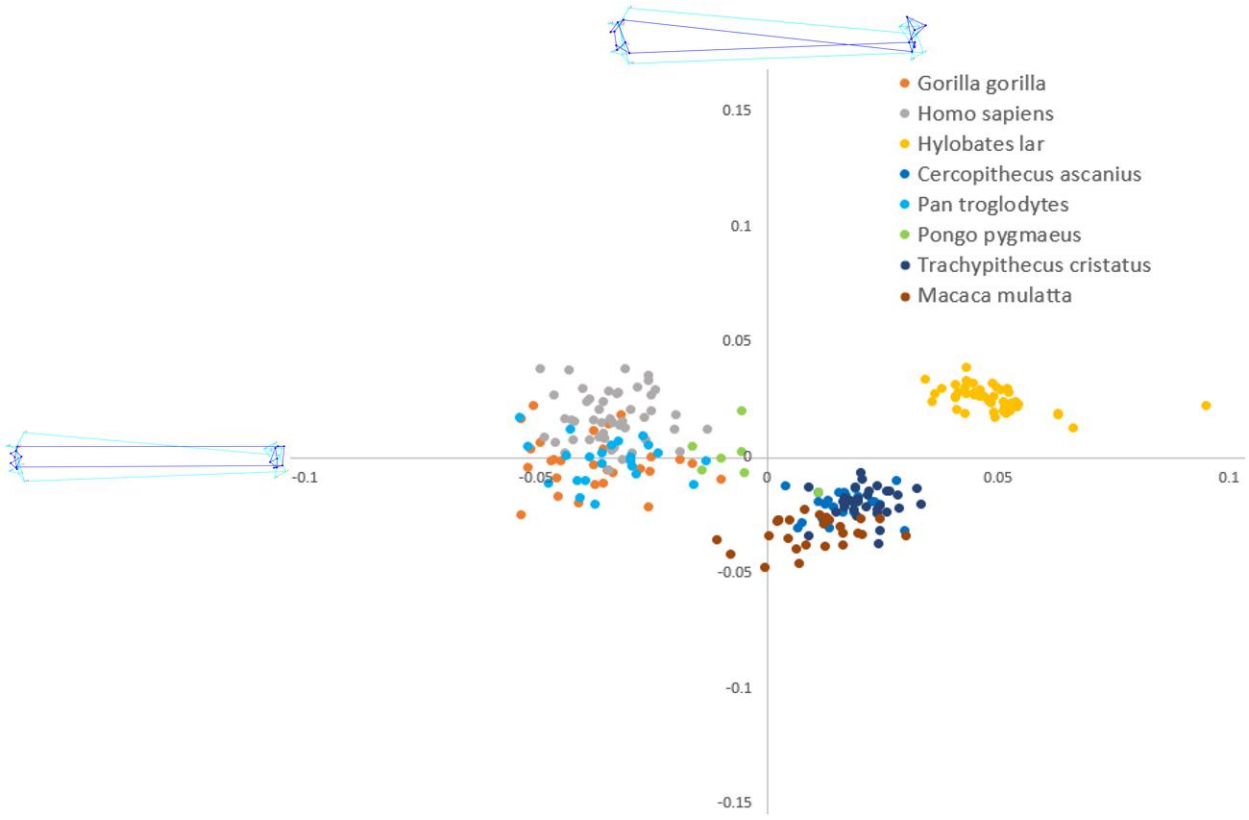

Figure 3.3. Interspecific humeral morphological variation PCA plot with wireframes, illustrating the major shape changes along each of the PCs. PC1 (x-axis) explains 55.18% of the variance, while PC2 (y-axis) explains 22.91% of the variance. The light blue wireframe illustrates the average shape transformation towards the negative end, while the dark blue wireframe illustrates the average shape towards the positive end.

Sexual Dimorphism

The results from the Procrustes ANOVAs for all taxa concerning clavicular ($F = 3.38$, p-value < 0.0001), scapular ($F = 2.74$, p-value < 0.0001), and humeral ($F = 3.63$, p-value < 0.0001) sexual dimorphism were significant which meant that at least one species must be sexually dimorphic for each of the bones and that further analysis of individual species required further investigation. Following the Procrustes ANOVA procedures for each individual species in MorphoJ (Klingenberg, 2011), the results revealed that there was sexual shape dimorphism

associated with four of the eight species included (see Table 3.1). Therefore, we can reject the null hypothesis that there is no clavicular, scapular, or humeral intraspecific sexual dimorphism. The results reveal that there is sexual dimorphism detectable in *Macaca mulatta* clavicles, but not for their scapulae or humeri. *Gorilla gorilla* had no sexual shape dimorphism associated with their clavicles, but had sexually dimorphic scapulae and humeri. Both *Homo sapiens* and *Trachypithecus cristatus* displayed sexual shape dimorphism for all three shoulder girdle bones.

Table 3.1. Within species clavicular, scapular, and humeral sexual dimorphism based on Procrustes ANOVA tests performed within each taxon.

	Clavicular sexual dimorphism	Scapular sexual dimorphism	Humeral sexual dimorphism
Cercopithecus ascanius	F=0.77, p=0.6991	F=0.93, p=0.5794	F=1.07, p=0.3510
Trachypithecus cristatus	F=4.03, p<0.0001	F=8.70, p<0.0001	F=2.83, p<0.0001
Gorilla gorilla	F=0.49, p=0.9390	F=3.22, p<0.0001	F=2.57, p<0.0001
Hylobates lar	F=1.32, p=0.1879	F=1.04, p=0.4054	F=0.45, p=0.9991
Macaca mulatta	F=2.01, p=0.0165	F=0.81, p=0.7615	F=0.54, p=0.9918
Pongo pygmaeus	F=1.33, p=0.2138	F=1.35, p=0.1195	F=0.70, p=0.9154
Homo sapiens	F=2.01, p=0.0154	F=2.75, p<0.0001	F=3.63, p<0.0001
Pan troglodytes	F=0.88, p=0.5777	F=0.63, p=0.9440	F=1.21, p=0.1736

Shape Differences Amongst Taxa

Procrustes ANOVA based on shape variation revealed that there was statistically significant clavicular, scapular, and humeral morphological disparity amongst species (see Table 3.2). Scapulae were associated with the most amount of morphological disparity amongst species ($F = 128.86$, $p < 0.0001$). Humeral morphological disparity ($F = 110.94$, $p < 0.0001$) was the second highest amongst the three shoulder girdle bones tested, while the clavicles were the least disparate, but differences amongst taxa were still statistically significant ($F = 29.52$, p-value < 0.0001). The pairwise Procrustes distances for clavicular morphological variance (see Table 3.3) revealed that the least amount of shape difference was between *Pan troglodytes* and *Homo sapiens*, while the most amount of variation was between *Hylobates lar* and *Homo sapiens*. The pairwise Procrustes distances for scapular morphological variance (see Table 3.4) revealed that the least amount of shape difference was between *Trachypithecus cristatus* and *Cercopithecus ascanius*, while the most amount of shape disparity was between *Hylobates lar* and *Homo sapiens* again. The pairwise Procrustes distances for humeral morphological variance (see Table 3.5) revealed, once again, that the least amount of shape difference was between *Trachypithecus cristatus* and *Cercopithecus ascanius*, while the most amount was between *Hylobates lar* and *Gorilla gorilla*, and also to a slightly lesser extent between *Hylobates lar* and *Pan troglodytes*/*Homo sapiens*.

Table 3.2. Clavicular, scapular, and humeral morphological variance amongst species.

Shoulder Girdle Bone	**Morphological Variance (amongst species)**
Clavicle	$F = 29.52$, p-value < 0.0001
Humerus	$F = 110.94$, p-value < 0.0001
Scapula	$F = 128.86$, p-value < 0.0001

Table 3.3. Clavicular pairwise Procrustes distances amongst species. The smallest pairwise differences between taxa are shown in blue, while the largest distances are shown in red.

	C. ascanius	*T. cristatus*	*G. gorilla*	*H. lar*	*M. mulatta*	*P. pygmaeus*	*H. sapiens*	*P. troglodytes*
C. ascanius		0.0637	0.0524	0.0583	0.0381	0.063	0.0765	0.0557
T. cristatus	<0.0001		0.0406	0.0609	0.0472	0.0525	0.0343	0.0398
G. gorilla	<0.0001	<0.0001		0.0753	0.0441	0.0741	0.0496	0.0314
H. lar	<0.0001	<0.0001	<0.0001		0.0438	0.0331	**0.0825**	0.0772
M. mulatta	<0.0001	<0.0001	<0.0001	<0.0001		0.0485	0.0678	0.0527
P. pygmaeus	<0.0001	<0.0001	<0.0001	<0.0001	<0.0001		0.0771	0.0742
H. sapiens	<0.0001	<0.0001	<0.0001	<0.0001	<0.0001	<0.0001		**0.0311**
P. troglodytes	<0.0001	<0.0001	0.001	<0.0001	<0.0001	<0.0001	<0.0001	

Table 3.4. Scapular pairwise Procrustes distances amongst species. The smallest pairwise differences between taxa are shown in blue, while the largest distances are shown in red.

	C. ascanius	*T. cristatus*	*G. gorilla*	*H. lar*	*M. mulatta*	*P. pygmaeus*	*H. sapiens*	*P. troglodytes*
C. ascanius		**0.1201**	0.229	0.2693	0.1263	0.2164	0.2409	0.2683
T. cristatus	<0.0001		0.2131	0.2638	0.1398	0.1494	0.2271	0.2402
G. gorilla	<0.0001	<0.0001		0.2484	0.2483	0.2067	0.1682	0.1269
H. lar	<0.0001	<0.0001	<0.0001		0.2045	0.245	**0.3441**	0.202
M. mulatta	<0.0001	<0.0001	<0.0001	<0.0001		0.1944	0.2949	0.2496
P. pygmaeus	<0.0001	<0.0001	<0.0001	<0.0001	<0.0001		0.2162	0.1877
H. sapiens	<0.0001	<0.0001	<0.0001	<0.0001	<0.0001	<0.0001		0.2295
P. troglodytes	<0.0001	<0.0001	<0.0001	<0.0001	<0.0001	<0.0001	<0.0001	

Table 3.5. Humeral pairwise Procrustes distances amongst species. The smallest pairwise differences between taxa are shown in blue, while the largest distances are shown in red (in this case three very similar large distances are highlighted.

	C. ascanius	*T. cristatus*	*G. gorilla*	*H. lar*	*M. mulatta*	*P. pygmaeus*	*H. sapiens*	*P. troglodytes*
C. ascanius		**0.0172**	0.0621	0.0581	0.021	0.0405	0.0637	0.0578
T. cristatus	<0.0001		0.0657	0.0544	0.0236	0.0419	0.0674	0.0608
G. gorilla	<0.0001	<0.0001		**0.0916**	0.0623	0.0381	0.0355	0.0194
H. lar	<0.0001	<0.0001	<0.0001		0.0714	0.0647	**0.084**	**0.0878**
M. mulatta	<0.0001	<0.0001	<0.0001	<0.0001		0.0484	0.0675	0.0566
P. pygmaeus	<0.0001	<0.0001	<0.0001	<0.0001	<0.0001		0.0431	0.0373
H. sapiens	<0.0001	<0.0001	<0.0001	<0.0001	<0.0001	<0.0001		0.0266
P. troglodytes	<0.0001	<0.0001	<0.0001	<0.0001	<0.0001	<0.0001	<0.0001	

The Non-metric Multidimensional Scaling (MDS) plots for each shoulder bone can be seen in Figures 3.4, 3.5, and 3.6. In each case 100% of the among-taxon Procrustes distance variation has been represented in only two axes, and the general pattern of similarity and differences among taxa mirrors what was observed in the PCA plots earlier. In the case of the clavicle (Fig. 3.4), the between-taxon differences are easier to see now that only taxon averages are being displayed. There is a clear separation between the Asian apes and the African great apes and humans along the major axis of variation, with all three monkey taxa lying intermediate to these two ape groups. The second axis separates the colobines and cercopithecines, and humans are also somewhat separated from chimpanzees and gorillas on this axis. The pattern for the scapular distances is similar to what was observed on the first two PC scores, with a clear separation between humans and gibbons on the major axis, with the other apes taxa lying somehwat intermediately (Fig. 3.5). The second axis also clearly distinguishes between the ape and cercopithecoid monkey taxa. In the case of the humerus (Fig. 3.6), the major axis distinguishes the gibbons from all other ape taxa, with the three monkey taxa being more similar to gibbons. The second axis separates the monkey taxa from the gibbons, and humans from the other great ape species.

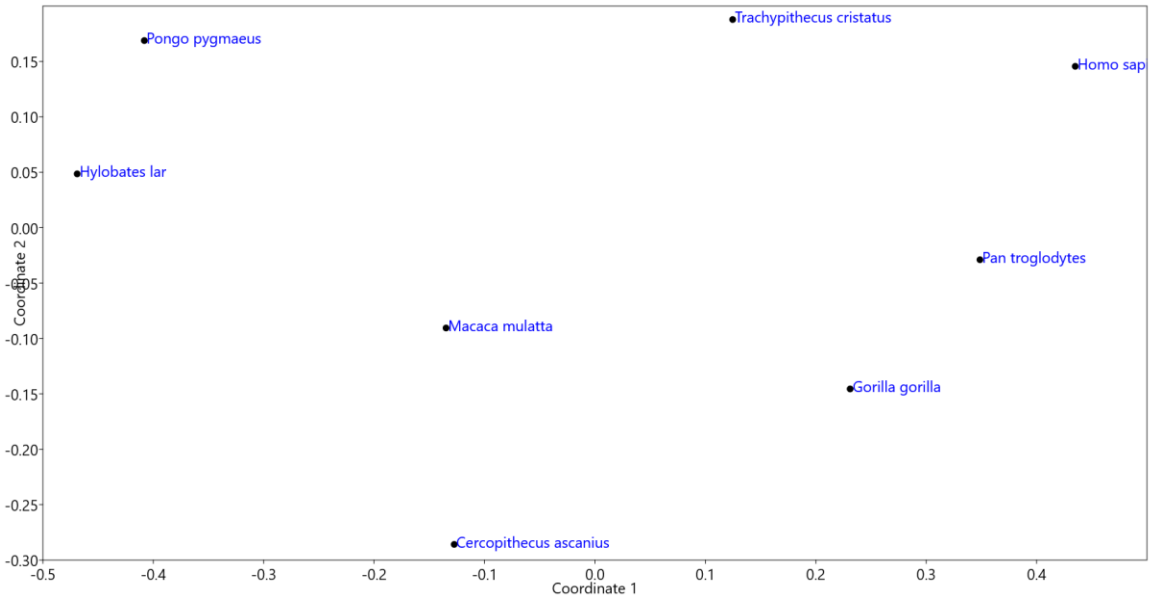

Figure 3.4. Non-metric Multidimensional Scaling (MDS) plot showing average among-taxon clavicular morphological distances. The major axis (x-axis) explains 89% of the total variance, while the second axis (y-axis) explains < 1%. Stress value = 0.0322 indicating that the distance matrix can be adequately represented in two dimensions.

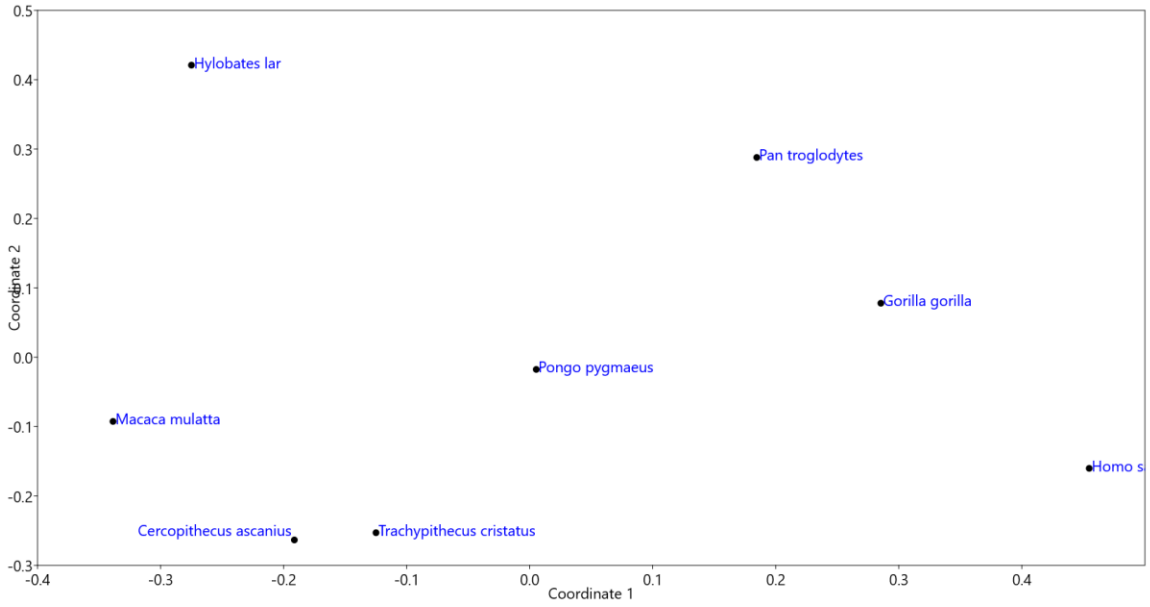

Figure 3.5. Non-metric Multidimensional Scaling (MDS) plot showing average among-taxon scapular morphological distances. The major axis (x-axis) explains 44% of the total variance, while the second axis (y-axis) explains 27%. Stress value = 0.07722 indicating that the distance matrix can be adequately represented in two dimensions.

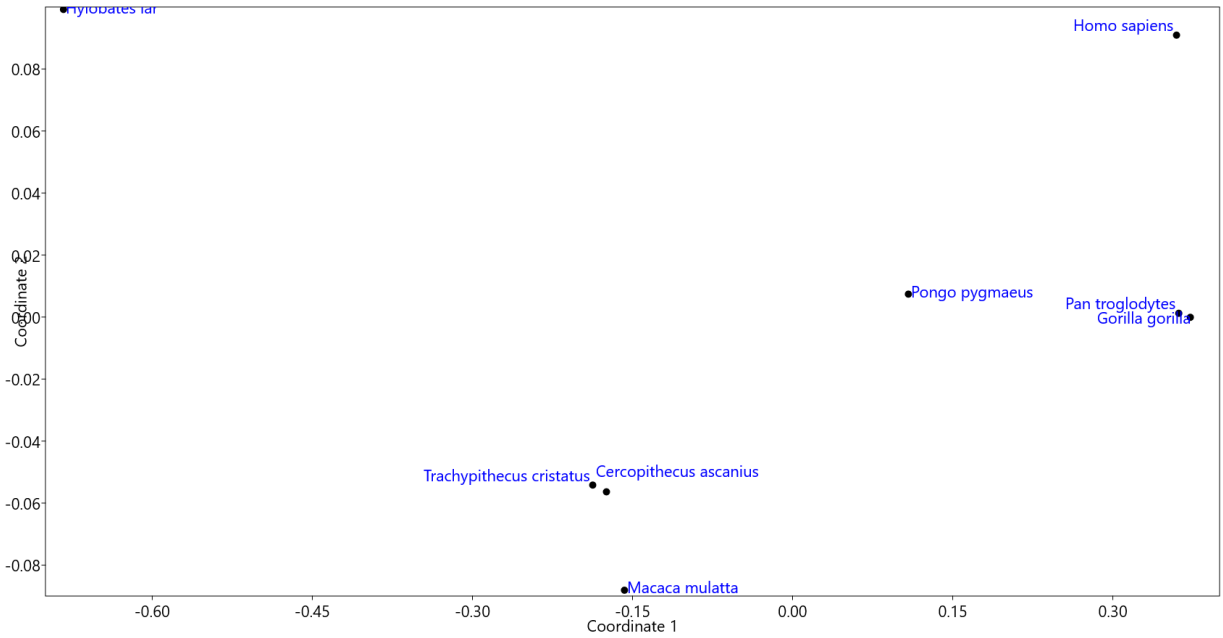

Figure 3.6. Non-metric Multidimensional Scaling (MDS) plot showing average among-taxon humeral morphological distances. The major axis (x-axis) explains 90% of the total variance, while the second axis (y-axis) explains 23%. Stress value = 0.06236 indicating that the distance matrix can be adequately represented in two dimensions.

Locomotion

After assessing each individual species' locomotion scores in accordance with the gravity and loading score scheme described in the Materials and Methods, a matrix (see Table 3.6), was created that represents the pairwise among-taxon distances associated with differences in locomotion among taxa. The resultant locomotion distance matrix was subjected to a Non-metric Multidimensional Scaling (MDS) analysis in Past 4.09 (Hammer, O., Harper, D.A.T., P.D., 2001) as a visual representation of the locomotor similarities and differences among taxa (see Figure 3.7). The x-axis primarily differentiates between the more arboreal and forelimb dominated (on left) and more terrestrial and hindlimb (on right), while the y-axis differentiates among the more arboreal and terrestrial quadrupeds.

Table 3.6. Locomotion distance quantification matrix.

	C. ascanius	*T. cristatus*	*G. gorilla*	*H. lar*	*M. mulatta*	*P. pygmaeus*	*H. sapiens*	*P. troglodyte*
C. ascanius		1	3.0413813	2.236068	1	1	3.6055513	2.0615528
T. cristatus	1		4.0311289	2	2	1.4142136	4.472136	3.0413813
G. gorilla	3.0413813	4.0311289		4.2720019	2.0615528	3.0413813	2.5	1
H. lar	2.236068	2	4.2720019		2.8284271	1.4142136	5.6568542	3.354102
M. mulatta	1	2	2.0615528	2.8284271		1.4142136	2.8284271	1.118034
P. pygmaeus	1	1.4142136	3.0413813	1.4142136	1.4142136		4.2426407	2.0615528
H. sapiens	3.605513	4.472136	2.5	5.6568542	2.8284271	4.2426407		2.6925824
P. troglodytes	2.0615528	3.0413813	1	3.354102	10118034	2.0615528	2.6925824	

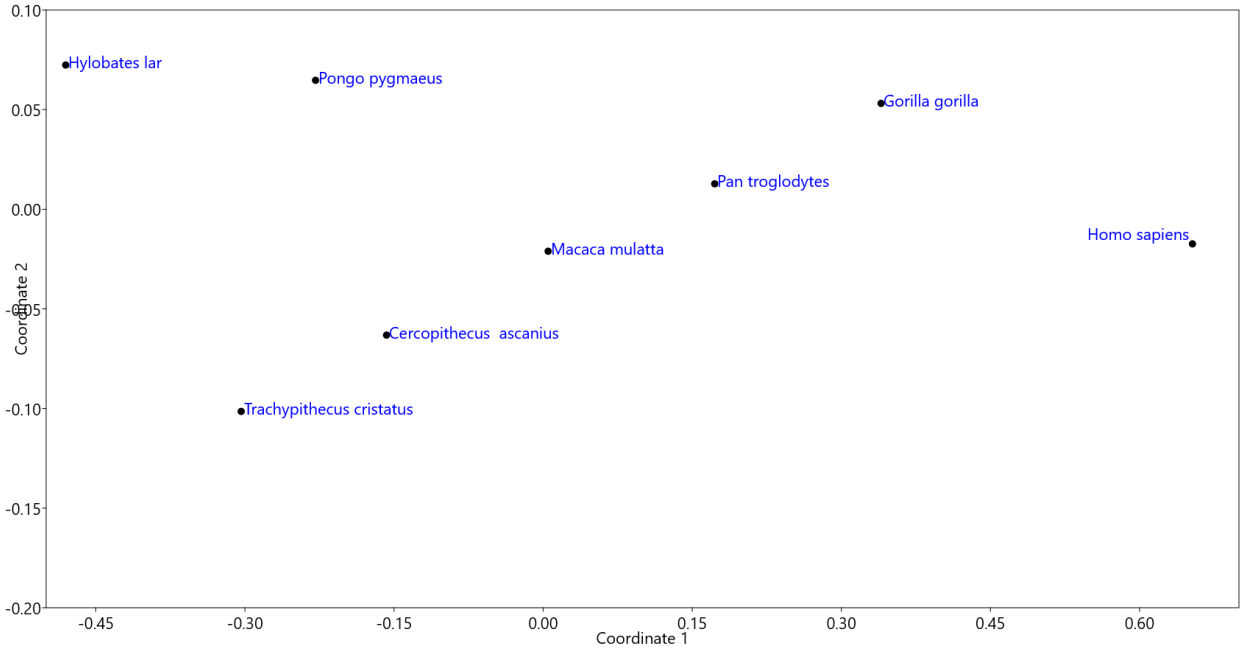

Figure 3.7. Non-metric Multidimensional Scaling (MDS) plot showing average among-taxon locomotor distances. The major axis (x-axis) explains 95% of the total variance, while the second axis (y-axis) explains 5%. Stress value = 0.04554 indicating that the distance matrix can be adequately represented in two dimensions.

Genetic Distance

The genetic distance quantifications matrix that was calculated based on the molecular phylogeny data from Perelman et al. (2011) can be seen below (see Table 3.7). The Non-metric Multidimensional Scaling (MDS) plot based on this genetic distance matrix can be seen below

(Fig. 3.8) and displays the relative genetic relatedness between taxa. The two major taxonomic groupings associated with the cercopithecoids and the hominoids are obvious, but the genetic variability within the hominoids is also obvious within the y-axis, with *Hylobates lar* having significant genetic distance from the other apes. The genetic relatedness among taxa was also visualized in the form of a neighbor-joining tree (Saitou and Nei, 1987) (Fig. 3.9), which allowed the confirmation that the known patterns of genetic relatedness among taxa could be reconstructed from the genetic distance matrix.

Table 3.7. Genetic distance quantification matrix.

	C. ascanius	***T. cristatus***	***G. gorilla***	***H. lar***	***M. mulatta***	***P. pygmaeus***	***H. sapiens***	***P. troglodytes***
C. ascanius		149.38	331.09	366.61	85.53	316.16	339.05	331.73
T. cristatus	149.38		354.01	389.53	162.37	339.08	361.97	354.65
G. gorilla	331.09	354.01		249.88	344.08	171.51	88.20	80.88
H. lar	366.61	389.53	249.88		379.6	234.95	257.84	250.52
M. mulatta	85.53	162.37	344.08	379.60		329.15	352.04	344.72
P. pygmaeus	316.16	339.08	171.51	234.95	329.15		179.47	172.15
H. sapiens	339.05	361.97	88.20	257.84	352.04	179.47		73.70
P. troglodytes	331.73	354.65	80.88	250.52	344.72	172.15	73.70	

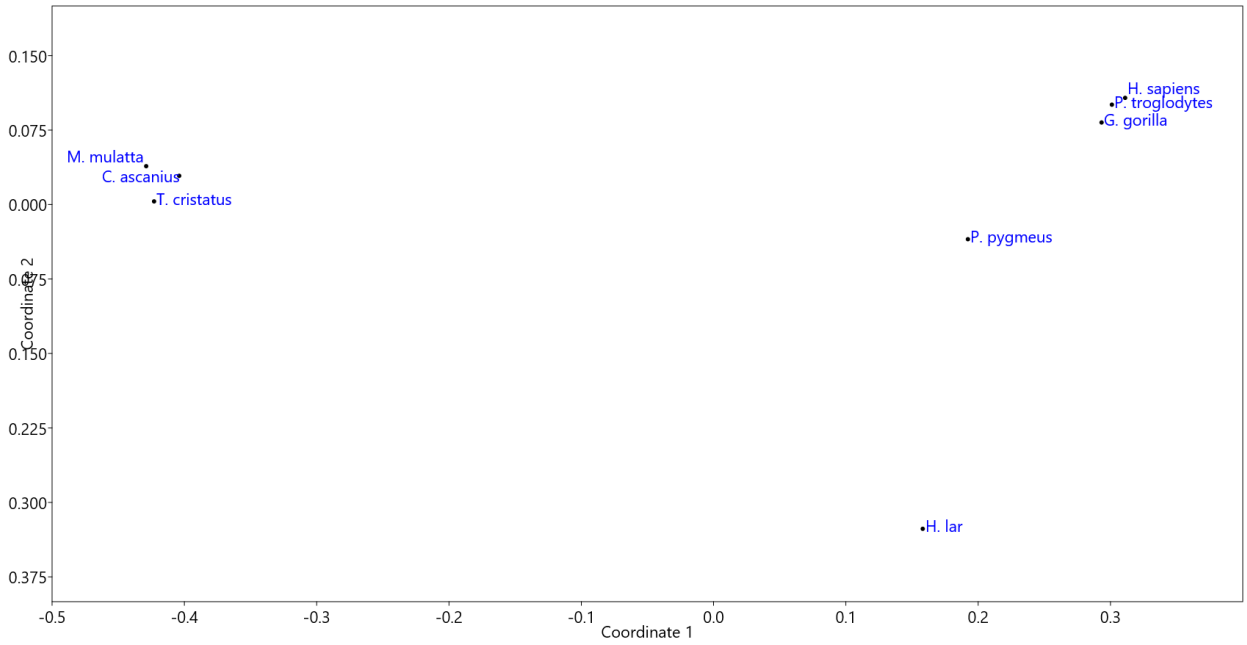

Figure 3.8. Non-metric Multidimensional Scaling (MDS) plot showing average among-taxon genetic distances. The major axis (x-axis) explains 92% of the total variance, while the second axis (y-axis) explains 8%. Stress value = 0 indicating that the distance matrix can be adequately represented in two dimensions.

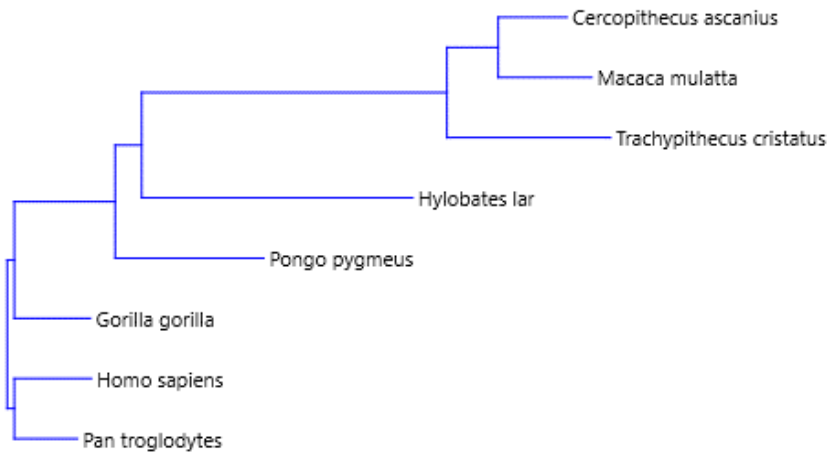

Figure 3.9. Neighbor-joining tree based on the genetic distance matrix.

Mantel and patrial Mantel tests

The correlation procedures conducted in PASSaGE v2 (Rosenberg, M.S., and C.D. Anderson, 2011) between the locomotion distances matrix and the clavicular, scapular, and humeral distance matrices revealed statistically significant correlations for all bones (see Table 3.8). The genetic distances matrix and the clavicular, scapular, and humeral variation distances matrices reveal statistically significant correlations for the scapulae and humeri, but not for the clavicle (see Table 3.8). The partial Mantel test displaying the correlation between the locomotion distances matrix and the clavicular, scapular, and humeral variation distances matrices, while holding the genetic distances matrix as a constant revealed statistically significant results for all correlations between locomotion and morphology (see Table 3.8).

Table 3.8. Correlation results from the series of Mantel's (1967) -tests. Significant correlations (r-values and two-tailed p-values) are bolded.

	Clavicular variation distances	Scapular variation distances	Humeral variation distances
Locomotion distances	**r=0.38895, p=0.036**	**r=0.53319, p=0.007**	**r=0.6316, p=0.004**
Genetic distances	r=0.07915, p=0.694	**r=0.56703, p=0.006**	**r=0.65031, p=0.003**
Genetic distances constant	**r=0.38215, p=0.047**	**r=0.53228, p=0.021**	**r=0.69055, p=0.008**

Chapter Four: Discussion

Sexual dimorphism

The results from the intraspecific clavicular, scapular, and humeral sexual dimorphism Procrustes ANOVA indicated statistically significant levels of sexual dimorphism present in four of the eight species, including two monkey and two ape taxa. *Pan troglodytes*, *Pongo pygmaeus*, *Hylobates lar*, and *Cercopithecus ascanius* did not have sexually dimorphic clavicles, scapulae, or humeri. Two of the sampled species, *Homo sapiens* and *Trachypithecus cristatus*, had sexually dimorphic clavicles, scapulae, and humeri, which means that both species have shoulder girdles that display sexual shape dimorphism in all bones. The *Gorilla gorilla* sample results indicated sexually dimorphic scapulae and humeri, but excluded significant results for their clavicles which is opposite of what we see regarding *Macaca mulatta*'s shoulder girdle bones. The *Macaca mulatta* sample results indicated that they have sexually dimorphic clavicles, but there is no sexual dimorphism associated with their scapulae or humeri. *Pan troglodytes*, *Pongo pygmaeus*, *Hylobates lar*, and *Cercopithecus ascanius* did not have sexually dimorphic clavicles, scapulae, or humeri. Taken together, these results suggest that we can reject the first null hypothesis ($H1_0$) that there is no intraspecific sexual shape dimorphism in the clavicle, scapular, or humerus. We accept the first alternative hypothesis ($H1_{A1}$) that there is interspecific sexual shape dimorphism in the clavicle, scapula or humerus due to the significant results indicating sexual dimorphism associated with *Homo sapiens*, *Trachypithecus cristatus*, *Gorilla gorilla*, and *Macaca mulatta*. Also, we can reject the second alternative hypothesis ($H1_{A2}$) that there is sexual shape dimorphism in the clavicle, scapula, and humerus of *Trachypithecus cristatus* only.

Many previous studies have suggested that dimorphism is caused by changes to male and female traits and that different ontogenetic trajectories can lead to dimorphism (e.g., Plavcan,

2001). Despite the extensive research on primate sexual dimorphism, but there have been only a few studies that include information about clavicles, scapulae, and humeri. A study by Taylor (1997) examined patterns of ontogeny and sexual size dimorphism in *Gorilla gorilla gorilla* and *Gorilla gorilla beringei* scapulae, humeri, femora, and ilia and suggested that gorillas are the most sexually dimorphic extant primate species. Results from the study indicated that there were sexual dimorphism and ontogenetic differences between the two *Gorilla* subspecies which may be associated with ecological variation (Taylor, 1997). While the present study looked at sexual shape dimorphism instead of sexual size dimorphism, *Gorilla gorilla* were also found to have sexually dimorphic scapulae and humeri, but the results do not suggest statistically significant sexual shape dimorphism in their clavicles. This was opposite to the pattern for *Macaca mulatta,* which had statistically significant sexual shape dimorphism associated with their clavicles, but did not have positive results for their scapulae and humeri. Although both taxa are associated with more terrestrial patterns of locomotion, *Gorilla gorilla* and *Macaca mulatta* have very distinct locomotor patterns and are phylogenetically quite distant, so not having similar patterns of shoulder girdle dimorphism would be expected.

The results obtained here for human sexual dimorphism patterns conform to recently published results on human pectoral girdle and pelvic girdle sexual dimorphism (Hudson and Langdon, 2023). They examined two human populations and accounted for sexual size dimorphism as well as shape. Hudson and Langdon (2023) concluded that human males have much broader pectoral regions than human females and that human females have broader pelvic regions than human males do, while also confirming that the results were not simply the result of scaling differences. The present study also concluded that there is statistically significant sexual shape dimorphism associated with all three bones of the pectoral girdle of *Homo sapiens*. However, it

should be noted that the results for the clavicle would not have statistically significant had a strict Bonferroni correction been applied (Table 3.1), while the results for the scapula and humerus are very statistically robust.

A previous study (Klier et al., 2021) found that *Trachypithecus cristatus* showed substantial sexual shape dimorphism in the clavicle, and this was confirmed in the present study also. According to Harding (2010), *Trachypithecus cristatus* is less sexually dimorphic compared to most other colobines, while Roonwal and Mohnot (1977) suggest that males are 11% larger than the females are. Moreover, the results also found significant sexual shape dimorphism in the scapula and humerus for *Trachypithecus* which means, like *Homo sapiens*, they have completely sexually dimorphic shoulder girdles. However, *Trachypithecus cristatus*, unlike *Homo sapiens*, would still have significant results for clavicular sexual shape dimorphism after a strict Bonferroni correction, suggesting that of all the species tested here, these colobines have the most consistent patterns of sexual shape dimorphism in the pectoral girdle. It is important to note that this study did not take *size* dimorphism into consideration for any of the analyses, which might explain why not all taxa showed significant patterns of sexual dimorphism.

Taxonomic Shape Disparity

The results from the Procrustes ANOVA testing differences in clavicular, scapular, and humeral morphological variance amongst species indicated that there are statistically significant differences among taxa for all three bones (see Table 3.2). The scapular among-species morphological variance ($F = 128.86$, p-value < 0.0001) was the highest potentially due to its relatively increased morphological complexity compared to the other shoulder girdle bones that were sampled. The humeral among-species morphological variance ($F = 110.94$, p-value < 0.0001) was the second highest, which is also potentially due to its relatively high morphological

complexity, especially when compared to primate clavicles. The clavicular among-species morphological variance ($F = 29.52$, p-value < 0.0001) was much less than both humeral morphological variance and scapular morphological variance potentially due to its relatively low morphological complexity. Even though the results showed much lower levels of among-species clavicular variation with significant overlap there were still clearly identifiable patterns of differences between the eight species in the plot of the first two Principal Components (Fig. 3.1). These results regarding clavicles makes sense when compared with results from other clavicular morphology variation studies (e.g., Voisin 2006). The PCA results reflect the statistical findings of the Procrustes ANOVAs in showing a much greater degree of among-taxon differentiation for the scapula (Fig. 3.2) and to a lesser extent for the humerus (Fig. 3.3. This means that we can reject the second null hypothesis ($H2_0$) that there is no intraspecific shape disparity in the clavicle, scapula, or humerus.

The comparison of Procrustes distances among all taxa also revealed patterns of morphological disparity between pairs of species. The greatest amount of clavicular morphological distance was between *Hylobates lar* and *Homo sapiens* (0.0825, $p < 0.0001$), which could potentially be due to their very different modes of locomotion, while the least amount of clavicular morphological distance was between *Homo sapiens* and *Pan troglodytes* (0.0311, $p < 0.0001$) (Table 3.3), which could potentially be due to their close phylogenetic relatedness. These among-taxon patterns are also reflected in the PCA plot shown in Figure 3.1. Also, the greatest amount of scapular morphological distance was between *Hylobates lar* and *Homo sapiens* (0.3441, $p < 0.0001$), but the least amount of clavicular morphological distance was between *Cercopithecus ascanius* and *Trachypithecus cristatus* (0.1201, $p < 0.0001$) (Table 3.4), which could potentially be due to both their similar locomotor patterns as well as their phylogenetic relatedness. Again,

this fits well with the pattern of taxonomic similarity and difference show in the PCA plot in Figure 3.2. The greatest humeral morphological distance was between *Hylobates lar* and *Gorilla gorilla* (0.0916, $p < 0.0001$), which could potentially be due to their very different locomotor patterns and social behaviors. The distances between *Hylobates lar* and *Pan troglodytes* (0.0878, $p < 0.0001$), and between gibbons and humans (0.084, $p < 0.0001$) were also large and noteworthy. This concurs with the patterns shown in the PCA plot in Figure 3.3., where humans, chimps and gorillas have a large amount of overlap at one end of PC1, with gibbons at the extreme other end of PC1. The least amount of humeral distance was between *Cercopithecus ascanius* and *Trachypithecus cristatus* (0.0172, $p < 0.0001$), mirroring the patterns seen in the scapular results (Table 3.5). These results indicate that we can reject the third alternative hypothesis ($H2_{A3}$) that there is between species shape disparity in the clavicle, scapula, or humerus but only for *Hylobates lar*.

Here appears to be clavicular, scapular, and humeral morphological disparity among all the taxa to a greater or lesser degree. However, there does appear to be substantial morphological difference between *Hylobates lar* and all of the other seven taxa, which does not seem surprising due to their substantially different pattern of locomotion within the catarrhine parvorder. *Hylobates lar* has a very unique form of ricochetal brachiating locomotion and is considered an arboreal true-brachiator (Strier, 2016), which is different than the other patterns of locomotion included here, such as arboreal quadrupedalim, terrestrial quadrupedalism, quadrumanous movements, knuckle-walking, or bipedalism. Another factor potentially driving the larger shoulder girdle morphological distances is that *Hylobates lar* is also genetically distant from all the other species (Table 3.7 and Figure 3.8). Even though *Hylobates lar* appears to be closer to the apes (especially *Pongo pygmaeus*), they are still significantly genetically distant from all taxa as shown in the MDS plot (see Figure 3.8) and in the genetic distance neighbor-joining tree (see Figure 3.9). *Hylobates lar*

clavicular morphology appears to be closest to *Pongo pygmaeus*, but they also appear to be closer in shape to the cercopithecines relative to the other four ape taxa which is potentially due to the cercopithecine association with arboreal or semi-arboreal quadrupedalism (see Figure 3.4). *Hylobates lar* scapular morphology appears to be distinct from all other taxa, but still closer to the cercopithecines, which may be due to their disassociation from the more terrestrial locomotor patterns of the African apes (see Figure 3.5). *Hylobates lar* humeral morphology appears to be far distant from all the other taxa and this is potentially due to *Hylobates lar*'s humeri having more elongated humeral shafts than any of the other taxa (see Figure 3.6). The greater shoulder girdle morphological disparities between *Hylobates* lar and the other apes relative to the cercopithecines could also potentially be due to hylobatid and cercopithecine evolutionary convergence.

Phylogenetic signal

The results of the Mantel test comparisons between morphological distance and genetic distance revealed statistically significant results for all bones except for the clavicle (Table 3.8), suggesting that the scapula and humerus, but not the clavicle reflect phylogenetic patterns to some extent. The MDS plot showing the average among-taxon genetic distances (see Figure 3.8) displays a different pattern than what is seen on the three bone's morphological relatedness MDS plots (see Figures 3.4, 3.5, and 3.6) by displaying an increase in genetic relatedness between *Hylobates lar* and the other apes, whereas the morphological variation MDS plots appear to show *Hylobates lar*'s shoulder girdle bones being morphologically closer to the monkeys. This is potentially a result of *Hylobates Lar*'s significantly increased use of the forelimbs relative to the other four ape species. As for the phylogenetic signals for the shoulder girdle bones, the scapula has the strongest signal (see Figure 3.5). The humerus also shows a significant phylogenetic signal, but there is much more overlap than is observed for the scapulae (Figure 3.3). Even though

phylogenetic signal is the least for the clavicles and there is significantly more overlap associated with the clavicle relative to the other two bones, there are still generally observable phylogenetic groupings (see Figure 3.1).

The lack of significant correlation with genetic distance for the clavicle is probably related to the wide disparity between the colobine and cercopithecine taxa, which lie intermediate to the Asian apes on one hand, and the African apes and humans on the other hand (Fig. 3.4). Hence, while some taxonomic signal is clear in the clavicle data it does not match what is expected based on phylogeny. Conversely, the scapula and humerus both show clear separation between the apes and the cercopithecines on one or more axes (Figs. 3.5-3.6), even if the exact pattern of taxonomic differences is not the same as it is in the genetic matrix. Therefore, taken together we can accept the first alternative hypothesis ($H2_{A1}$) that there is interspecific shape disparity in the clavicle, scapula, and humerus associated with phylogeny.

Locomotion

Results from the Mantel's (1967) -tests suggest a statistically significant correlation between locomotor function (as measured here) and clavicular, scapular, and humeral among-taxon distances, which indicates that shoulder girdle bone morphological variance is associated with differences in locomotor patterns amongst all the sampled taxa (see Table 3.8). This holds true even when the effects of phylogeny are controlled for in partial Mantel test with the genetic distances held constant. There are significant locomotion differences and similarities associated with the eight different taxa. There are varying phylogenetic distances concerning the different species, but the two most significant phylogenetic groupings are between the three monkeys and the five different ape species. Even though there is a strong taxonomic signal associated with each species, all three PCAs (see Figure 3.1, Figure 3.2, and Figure 3.3) appear to show two primary

morphological groupings where one is comprised of *Cercopithecus ascanius*, *Trachypithecus cristatus*, *Macaca mulatta* and Hylobates lar and the other grouping comprised of *Homo sapiens*, *Pan troglodytes*, *Gorilla gorilla*, and *Pongo pygmaeus*. However, *Hylobates lar* does appear to be distinct from both major taxonomic groupings, even though they are apes. This is likely due to their very unique suspensory locomotor capabilities which are closer to some new world monkeys, but due to *Hylobates lar*'s taxonomic classification as an ape, they do not have tails like platyrrhines so they are true brachiators (Strier, 2016). These phylogenetic groupings regarding primate shoulder girdle bone morphological variance appear to be much weaker on the clavicular morphological variance PCA relative to the other two shoulder girdle bone's PCAs. This is likely due to clavicular morphological complexity being much less than scapular, or humeral morphological complexity. The MDS plot showing the average among-taxon locomotor distances (Figure 3.7) show a similar pattern that is seen in the morphology MDS plots for all three of the shoulder girdle bones (see Figures 3.4, 3.5, and 3.6). *Hylobates lar*'s locomotion pattern appears to be more similar to clavicular, scapular, and humeral morphological distance patterns than they do to the genetic distance pattern (see Figure 3.8). This is potentially due to *Hylobates lar*'s phylogenetic association with the apes, but a locomotor pattern that involves the forelimbs significantly more than is observed in the other ape taxa. The locomotion results indicate that we can accept the second alternative hypothesis ($H2_{A2}$) that there is interspecific shape disparity in the clavicle, scapula, or humerus associated with differences in locomotion.

Limitations

There were a few limitations encountered during the course of this project that potentially affected the robustness of the results obtained and, had they been absent, could have increased our knowledge regarding primate clavicles, scapulae, and humeri. One of the issues encountered

includes limitations on the sample sizes that were available for inclusion in the analyses. For example, there would likely be increased benefit in having larger sample sized for each of the eight species. This is especially true regarding the *Pongo pygmaeus* sample which only consisted of four females and three males. Of course, if more specimens were included in the study, there would likely be increased accuracy concerning statistical analyses. Another issue with the samples was that only catarrhine parvorder species were included due to a lack of availability of samples from other parvorders. There also were limitations regarding the quality of some of the 3D scanned images that were previously collected from several different locations. Unusable scans were usually associated with holes that prevented landmarks from being placed in their required locations and were usually discovered during the landmarking process. In the instances when there were unreliable scans that were collected locally, the specimens were located and re-scanned until usable scans were produced. In the instances when there were unreliable scans that were collected from satellite collections, the specimens were unable to be re-scanned and were subsequently excluded from the analyses.

Conclusion

The information derived from this study revealed significant information regarding primate clavicular, scapular, and humeral morphological variation including sexual shape dimorphism, which is not uniform across all taxa. Due to the limitations of this study, there are future studies that can be pursued. Research conducted by Makandar (2011) concluded that left side clavicles are longer than right side clavicles and that there are more lateral angle degrees associated with left side clavicles than right side clavicles for both male and female humans. There would likely be benefit in including handedness information (especially in humans) in future research which could potentially increase knowledge regarding any relationship between

handedness and clavicular, scapular, or humeral morphology and to test if osteological plasticity may be a confounding factor. The inclusion of a broader taxonomic sample would be desirable for further primate shoulder girdle morphological variance research. The inclusion of platyrrhine samples would have been especially desirable in order to potentially reveal comparative shoulder girdle morphological disparities as well as to investigate potential sexual shape dimorphism within new world monkey species. The analysis of platyrrhine shoulder girdle bones could potentially reveal important information regarding potential convergence in locomotion between *Hylobates lar* and certain platyrrhines that are associated with semi-brachiation locomotor patterns. It would also be desirable if non-simiiformes could have been included, such as using lemuriformes and tarsiformes, but resources needed to gather additional samples were unfortunately limited and they were not able to be included in this study.

Research conducted by Agosto and Auerbach (2021) suggested that there was evolutionary covariance between the pectoral girdle, the basicranium, and the pelvic girdle. As such, there would likely be added benefit in conducting more shoulder girdle morphology research that included data derived from the pelvic girdle in order to increase our knowledge base regarding exact evolutionary processes that affect the morphology of these two skeletal regions. A recent study by Hudson and Langdon (2023) suggested that primate pectoral girdle sexual dimorphism is influenced by adaptive forces affecting both sexes differently and that observed differences were not influenced by scaling factors. Additional pectoral/pelvic girdle covariation data regarding sexual dimorphism could potentially increase our knowledge base concerning allometry and size dimorphism. There are also several behavioral factors that could potentially be affecting primates shoulder girdle morphology that were beyond the scope of this project but would be desirable for inclusion in future research. Some of these behaviors include feeding differences amongst species

that require different abilities, techniques, and cognition to perform. Early primate strategies that were adopted to accommodate arboreal dietary challenges likely significantly influenced primate evolution (Milton, 1993). It would not be unreasonable to hypothesize that there may be correlations between primate dietary feeding practices and osteological morphological variance, especially regarding the shoulder girdle and forelimbs. Another primate behavioral factor that may potentially affect shoulder girdle morphology is infant care both among species as well as potentially affecting intraspecific sexual shape dimorphism. According to Bercovitch and Ziegler (2002), individuals evolved an adaptive flexibility that enables them to adjust mating and parenting efforts to accommodate their social structures which ultimately facilitates different mating strategies that increase biological fitness. The diverse mating and parenting strategies associated with the primate order could have potentially, from an evolutionary perspective, influenced their shoulder girdle morphologies.

Aiello, Leslie, and Christopher Dean. *An introduction to human evolutionary anatomy*. Academic Press, 1990.

Agosto, Elizabeth R., and Benjamin M. Auerbach. "Integration, Evolvability, and Constraint within the Primate Functional Shoulder Complex." *The FASEB Journal* 32 (2018): 364-2.

Agosto, Elizabeth R., and Benjamin M. Auerbach. "Evolvability and constraint in the primate basicranium, shoulder, and hip and the importance of multi-trait evolution." *Evolutionary Biology* 48, no. 2 (2021): 221-232.

Agosto, Elizabeth R., and Benjamin M. Auerbach. "Morphological integration and evolutionary potential of the primate shoulder: Variation among taxa and implications for genetic covariances with the basicranium, pelvis, and arm." *Journal of Human Evolution* 169 (2022): 103221.

Arias-Martorell, Julia, Josep Maria Potau, Gaelle Bello-Hellegouarch, and Alejandro Perez-Perez. "Like father, like son: assessment of the morphological affinities of AL 288–1 (A. afarensis), Sts 7 (A. africanus) and Omo 119–73–2718 (Australopithecus sp.) through a three-dimensional shape analysis of the shoulder joint." *Plos one* 10, no. 2 (2015): e0117408.

Arias-Martorell, Julia. "The morphology and evolutionary history of the glenohumeral joint of hominoids: A review." *Ecology and Evolution* 9, no. 1 (2019): 703-722.

Baab, Karen L., Kieran P. McNulty, and F. James Rohlf. "The shape of human evolution: a geometric morphometrics perspective." *Evolutionary Anthropology: Issues, News, and Reviews* 21, no. 4 (2012): 151-165.

Bain, Gregory Ian, Joideep Phadnis, Eiji Itoi, Giovanni Di Giacomo, Hiroyuki Sugaya, David H. Sonnabend, and James McLean. "Shoulder crane: a concept of suspension, stability, control and motion." *Journal of ISAKOS* 4, no. 2 (2019): 63-70.

Barros, A. P. "Ontogeny, phylogeny and functional morphology of the hominoid shoulder girdle." PhD diss., UCL (University College London), 2014.

Bercovitch, Fred B., and Toni E. Ziegler. "Current topics in primate socioendocrinology." *Annual Review of Anthropology* 31, no. 1 (2002): 45-67.

Chan, Lap Ki. "The range of passive arm circumduction in primates: do hominoids really have more mobile shoulders?." *American Journal of Physical Anthropology: The Official Publication of the American Association of Physical Anthropologists* 136, no. 3 (2008): 265-277.

Conaway, Mark A. "Quantification of integration in the hominoid postcranium in reference to evolutionary history and functional independence." PhD diss., State University of New York at Buffalo, 2021.

Corruccini, Robert S., and Russell L. Ciochon. "Morphometric affinities of the human shoulder." *American Journal of Physical Anthropology* 45, no. 1 (1976): 19-37.

Cunningham, Ian Stacy. "Shoulder morphology in four species of New World primate: Possible links to foraging behavior." PhD diss., University of Colorado at Boulder, 2005.

Polyga (2021). FlexScan3D.

Gebo, Daniel L., and Colin A. Chapman. "Positional behavior in five sympatric Old World monkeys." *American Journal of Physical Anthropology* 97, no. 1 (1995): 49-76.

Green, David J., and Zeresenay Alemseged. "Australopithecus afarensis scapular ontogeny, function, and the role of climbing in human evolution." *Science* 338, no. 6106 (2012): 514-517.

Green, David J., Ted A. Spiewak, Brielle Seitelman, and Philipp Gunz. "Scapular shape of extant hominoids and the African ape/modern human last common ancestor." *Journal of Human Evolution* 94 (2016): 1-12.

Hammer, O., Harper, D.A.T., P.D. 2001, PAST: Paleontological Statistics software package for education and data analysis. Palaeontologia Electronica 4(1): 9pp.

Harding, Lee E. "Trachypithecus cristatus (Primates: Cercopithecoidea)." *Mammalian Species* 42, no. 862 (2010): 149-165.

Holliday, Trenton W., and Lukáš Friedl. "Hominoid humeral morphology: 3D morphometric analysis." *American journal of physical anthropology* 152, no. 4 (2013): 506-515.

Hudson, Daphne R., and John H. Langdon. "Sexual dimorphism and ancestral variation in the pectoral and pelvic girdles of modern humans." *Homo: Internationale Zeitschrift fur die Vergleichende Forschung am Menschen* (2023).

INUZUKA, Norihisa. "Evolution of the Shoulder Girdle with Special Reference to the Problems of the Clavicle." *Journal of the Anthropological Society of Nippon* 100, no. 4 (1992): 391-404.

Ki-Kydd, Kimarnie, and Philip John Piper. "Identification of morphological variation in the humeri of Bornean primates and its application to zooarchaeology." *Archaeofauna* 13, no. 85 (2004): e95.

Klier, Kevin, Evan Simons, Noreen von Cramon-Taubadel. "A geometric morphometric analysis of the primate clavicle." *American Associated of Biological Anthropology poster presentation*, 2021.

Kagaya, Miyuki. "Glenohumeral joint surface characters and its relation to forelimb suspensory behavior in three ateline primates, Ateles, Lagothrix, and Alouatta." *Anthropological Science* 115, no. 1 (2007): 17-23.

Wiley, D.F. (2006). Landmark editor. Davis: University of California.

Larson, Susan G. "Shoulder morphology in early hominin evolution." *The paleobiology of Australopithecus* (2013): 247-261.

Makandar, UK, Kulkarni, P.R., and Surykar, A.N. "Identification of sex and race from the adult clavicle in South India." *Indian Journal of Forensic Medicine Toxicology* 5, no. 1 (2011): 48.

Mantel, Nathan. "Ranking procedures for arbitrarily restricted observation." *Biometrics* (1967): 65-78.

Melillo, Stephanie, Philipp Gunz, Hélène Coqueugniot, Stefan Reske, and Jean-Jacques Hublin. "Structural effects of variation in the human clavicle." *American Journal of Physical Anthropology* 168, no. 4 (2019): 687-704.

Milton, Katharine. "Diet and primate evolution." *Scientific American* 269, no. 2 (1993): 86-93.

Klingenberg, C. P. (2011). MorphoJ: an integrated software package for geometric morphometrics. Molecular ecology resources, 11(2), 353-357.

Perelman, Polina, Warren E. Johnson, Christian Roos, Hector N. Seuánez, Julie E. Horvath, Miguel AM Moreira, Bailey Kessing et al. "A molecular phylogeny of living primates." *PLoS genetics* 7, no. 3 (2011): e1001342.

Plavcan, J. Michael. "Sexual dimorphism in primate evolution." *American Journal of Physical Anthropology* 116, no. S33 (2001): 25-53.

Polyga (2021). FlexScan3D.

Preuschoft, Holger, Bianca Hohn, Heike Scherf, Manuela Schmidt, Cornelia Krause, and Ulrich Witzel. "Functional analysis of the primate shoulder." *International Journal of Primatology* 31, no. 2 (2010): 301-320.

Püschel, Thomas A., and William I. Sellers. "Standing on the shoulders of apes: analyzing the form and function of the hominoid scapula using geometric morphometrics and finite element analysis." *American journal of physical anthropology* 159, no. 2 (2016): 325-341.

Roonwal, Mithan Lal, and S. M. Mohnot. *Primates of South Asia: ecology, sociobiology, and behavior*. Harvard University Press, 1977.

Rosenberg, M.S., and C.D. Anderson, 2011 PASSaGE: Pattern Analysis, Spatial Statistics, and Geographic Exegesis. Version 2. Methods in Ecology and Evolution 2(3):229-232.

Saitou, Naruya, and Masatoshi Nei. "The neighbor-joining method: a new method for reconstructing phylogenetic trees." *Molecular biology and evolution* 4, no. 4 (1987): 406-425.

Schmidt, Manuela, and Cornelia Krause. "Scapula movements and their contribution to three-dimensional forelimb excursions in quadrupedal primates." In *Primate locomotion: Linking field and laboratory research*, pp. 83-108. New York, NY: Springer New York, 2010.

K.E. Sears, T. D. Capellini and R. Diogo. *Evolution* 2015 Vol. 69 Issue 10 Pages 2543-2555.

Sonnabend, D. H., and A. A. Young. "Comparative anatomy of the rotator cuff." *The Journal of bone and joint surgery. British volume* 91, no. 12 (2009): 1632-1637.

Squyres, Nicole, and Valerie Burke DeLeon. "Clavicular curvature and locomotion in anthropoid primates: A 3D geometric morphometric analysis." *American Journal of Physical Anthropology* 158, no. 2 (2015): 257-268.

Strier, Karen B. *Primate behavioral ecology*. Routledge, 2016.

Taylor, Andrea B. "Relative growth, ontogeny, and sexual dimorphism in Gorilla (Gorilla gorilla gorilla and G. g. beringei): Evolutionary and ecological considerations." *American Journal of Primatology* 43, no. 1 (1997): 1-31.

Taylor, Andrea B., and Dennis E. Slice. "A geometric morphometric assessment of the relationship between scapular variation and locomotion in African apes." *Modern morphometrics in physical anthropology* (2005): 299-318.

Vanhoof, Marie JM, Timo van Leeuwen, and Evie E. Vereecke. "The forearm and hand musculature of semi-terrestrial rhesus macaques (Macaca mulatta) and arboreal gibbons (Fam. Hylobatidae). Part I. Description and comparison of the muscle configuration." *Journal of Anatomy* 237, no. 4 (2020): 774-790.

Voisin, Jean-Luc. "Clavicle, a neglected bone: morphology and relation to arm movements and shoulder architecture in primates." *The Anatomical Record Part A: Discoveries in Molecular, Cellular, and Evolutionary Biology: An Official Publication of the American Association of Anatomists* 288, no. 9 (2006): 944-953.

Yamanaka, Atsushi, Harumoto Gunji, and Hidemi Ishida. "Curvature, length, and cross-sectional geometry of the femur and humerus in anthropoid primates." *American Journal of Physical Anthropology: The Official Publication of the American Association of Physical Anthropologists* 127, no. 1 (2005): 46-57.

Young, Nathan M. "Function, ontogeny and canalization of shape variance in the primate scapula." *Journal of Anatomy* 209, no. 5 (2006): 623-636.

Young, Nathan M. "A comparison of the ontogeny of shape variation in the anthropoid scapula: functional and phylogenetic signal." *American Journal of Physical Anthropology: The Official Publication of the American Association of Physical Anthropologists* 136, no. 3 (2008): 247-264.

Young, N.M., Wagner, G.P., Hallgrímsson, B., 2010. Development and the evolvability of human limbs. Proceedings of the National Academy of Sciences. 107, 3400–3405.

Young, Nathan M., and Benedikt HallgrÍmsson. "Serial homology and the evolution of mammalian limb covariation structure." *Evolution* 59, no. 12 (2005): 2691-2704.

White, Tim D., and Pieter Arend Folkens. *The human bone manual*. Elsevier, 2005.